HOKKAIDO UNIVERSITY

Title	Origin of Calc-Alkaline Andesite from Oshima-Ōshima Volcano, North Japan
Author(s)	Yamamoto, Masatsugu
Citation	北海道大学理学部紀要, 21(1), 77-131
Issue Date	1984-02
Doc URL	http://hdl.handle.net/2115/36726
Type	bulletin (article)
File Information	21_1_p77-131.pdf

Instructions for use

Hokkaido University Collection of Scholarly and Academic Papers : HUSCAP

Jour. Fac., Sci., Hokkaido Univ., Ser. IV,
vol. 21, no. 1, Feb., 1984, pp. 77-131.

ORIGIN OF CALC-ALKALINE ANDESITE FROM OSHIMA-ŌSHIMA VOLCANO, NORTH JAPAN

by

Masatsugu Yamamoto

(with 11 tables and 34 text-figures)

Abstract

Oshima-Ōshima volcanic island, a triple stratovolcano, is situated off the Japan sea coast, north Japan. The volcanic edifice consists of lavas and pyroclastics, about 30 vol% of calc-alkaline andesite and 70% of alkali olivine basalt. The andesite and basalt are intimately associated with each other, even within a single cycle of eruption as in the recorded eruption in 1741-1742.

Most of andesite and some basalt contain ultramafic and mafic inclusions which show a typical cumulate texture. The occurrence, texture and chemistry of minerals of these inclusions may have played an important role in fractional crystallization of the basaltic magma. A gradual change in modal contents of minerals is observed in the inclusions. Mg/Mg + Fe ratio of olivine, clinopyroxene and amphibole decreases from dunite to hornblende gabbro. Consequently, the crystallization sequence of the inclusions is inferred as follows: dunite → wehrlite → olivine clinopyroxenite → clinopyroxenite → hornbledite → hornblende gabbro.

The variation in major and trace elements of the volcanic rocks seems to result from successive fractionation of these inclusions from the basaltic magma. The trend from picritic basalt to felsic basalt is interpreted as due to the successive removal of dunite, wehrlite and clinopyroxenite (first removal), whereas that from the felsic basalt to andesite as due to the successive removal of hornblendite and hornblende gabbro (second removal). The first removal results in a considerable increase in Al_2O_3 content with a little SiO_2 enrichment of residual liquid, whereas the second removal leads to a constant Al_2O_3 content with a considerable SiO_2 enrichment. These chemical variations in the residual liquid reflect on the chemistry of clinopyroxenes in the inclusions.

The phase relationships in the basalt-andesite magma and the comparison of mineral chemistry between the inclusions and their host rocks suggest that the dunite fractionation from the primary magma took place under hydrous condition at higher pressure, whereas the subsequent fractionation proceeded under hydrous condition at low pressure. The variation in the volcanic rocks from alkaline basalt to calc-alkaline adnesite, therefore, is considered to be caused by amphibole fractionation from the felsic basalt under hydrous condition at shallower place in the continental crust.

The Quaternary volcanic rocks in the Notheast Honshū Arc vary markedly in the chemistry from the Nasu Volcanic Zone (Pacific side) to the Chōkai Volcanic Zone (Japan Sea side). The rocks of the Chōkai Zone including Oshima-Ōshima volcano are higher in alkali content than those of the Nasu Zone. Alkali content as well as H_2O content are considered to be important factors for the stability of amphibole. High alkali and H_2O contents are favorable to the fractionation of amphibole from the basaltic magma at the early stage of differentiation. In the Nasu Zone, common hornblende is rarely found in dacite whereas in the Chōkai Zone, pargasite occurs frequently in andesite, even in basalt. Thus, the calc-alkaline andesite from the Chōkai Zone may be originated from the basaltic magma through amphibole fractionation.

Introduction

Volcanism along the inner zone of the North Honshū Arc, Japan, has been active since the Miocene and many Quaternary volcanoes have been produced (Text-fig. 1).

Contribution from the Department of Geology and Mineralogy, Faculty of Science, Hokkaido University, No. 1833.

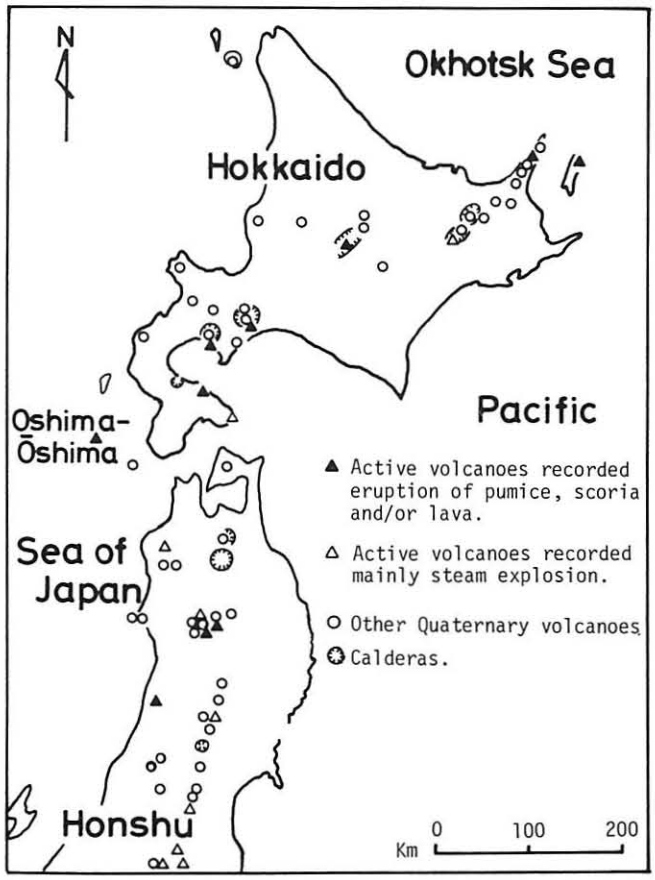

Text-fig. 1 Index map showing the location of Oshima-Ōshima Island.

The distribution of volcanoes and the existence of a deep-sea trench and active seismicity, the focal plane of which dips under the marginal sea, indicates that the North Honshū Arc has similar tectonic features to the double island arcs of the circum-Pacific belt.

As in other island arcs, the Quaternary volcanic rocks in this area are grouped in a basalt-andesite-dacite-rhyolite suite, of which andesite and dacite of the calc-alkaline series are generally abundant. These rocks vary markedly in nature from the Pacific side (calcic and low-potassic) to the Japan Sea side (more alkalic and high-potassic). High-alumina basalt or alkali olivine basalt are associated with the calc-alkaline rocks in many volcanoes (Kawano et al., 1961; Katsui et al., 1978). The calc-alkaline volcanic rocks are generally recognized as dominant rocks in island arcs, continental margins and other orogenic belts, hence their origin has become one of the principal problems of magmatism in orogenic belts.

During the past twenty years, geological and petrographical studies on Oshima-Ōshima Volcano have been carried out by Kuno (1936), Katsui and Satoh (1970), Yamamoto (1977), Yamamoto et al. (1977), Yamamoto (1978), and Katsui et al.

(1979). These results indicate that Oshima-Ōshima Volcano belongs to the Chōkai Volcanic Zone, and that the rocks are composed mainly of alkali olivine basalt and hornblende-pyroxene andesite of the calc-alkaline series, the latter of which is characterized by the presence of groundmass orthopyroxene and a variation trend of non iron enrichment. The basalt and andesite from Oshima-Ōshima are intimately associated with each other, even within a single cycle of eruption as in the recorded eruption in 1741-1942 (Katsui and Yamamoto, 1981). Almost continuous variation curves of major elements can be traced from the basalt to andesite without notable break. Mafic and ultramafic inclusions that occur in the andesite may also prove integral in explaining the genesis of calc-alkaline andesite.

The present study involves geological and petrographical investigation of Oshima-Ōshima Volcano, along with chemical analyses of the rocks and their constituent minerals. The principal problems addressed are:

(1) Petrogenetic relation between the volcanic rocks
(2) Crystallization of basaltic magma, and
(3) Origin of the calc-alkaline andesite of Oshima-Ōshima Volcano.

Geology

Oshima-Ōshima, a small volcanic island in the Sea of Japan, is located at Lat. 41°30′N and Long. 139°22′E (Text-fig. 1). This island is composed of a triple stratovolcano of basalt and andesite, and belongs to the Chōkai Volcanic Zone. The volcanic island has been dormant for the past two centuries, but had been active during 50 years from 1741 to 1790. The geology and volcanic history of the island have been studied by Katsui and Satoh (1970), Katsui et al. (1977), Yamamoto et al. (1977), and Katsui and Yamamoto (1981).

Volcanic topography

Oshima-Ōshima is situated 55 km off the western coast of the Oshima Peninsula, southwestern Hokkaido (Test-fig. 1). The island of Oshima-Ōshima is 4 km long in an E-W direction and 3.5 km wide, having an outline of an equilateral triangle whose apex is on the eastern side. The bathymetric chart shows that the volcanic body is on the eastern side of the Matsumae Plateau and has a submerged base, 12 km in diameter, from which the summit (737 m above sea level) rises 1,700-1,900 m (Katsui and Satoh, 1970). The slope of the volcanic edifice below sea level dips gently 10° to 15° whereas that above the sea level dips more steeply at 30° to 40°. There is no surface water, so no stream erosion has taken place anywhere. The island has long remained uninhabited due to the paucity of fresh water.

Geology

The island of Oshima-Ōshima consists of a triple stratovolcano (Text-fig. 2). The eastern part of the island is occupied by Higashi-yama which surrounds a caldera 200 m deep from the top of its eastern rim. The western part of the caldera is complete-

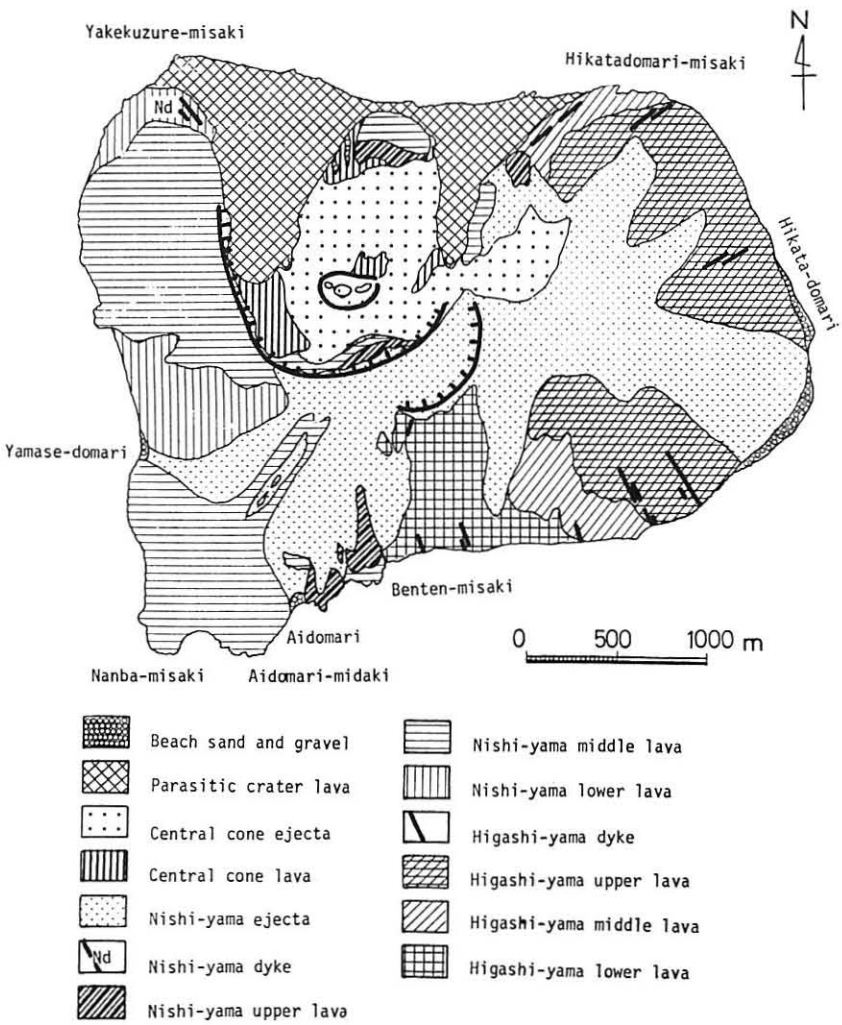

Text-fig. 2 Geologic map of Oshima-Ōshima Island.

ly covered by the lavas of the Nishi-yama which in turn encircles a caldera 1.3 km across and more than 160 m deep from the top of its southern rim. The northern rim of the Nishi-yama somma is absent. Accordingly the Nishi-yama somma is a horseshoe-shaped caldera. Within the caldera lies a central cone with a summit crater 250 × 300 m in diameter and 70 m in depth, rising 200 m from its base. The Central cone lavas and the parasitic crater lavas completely cover the Nishi-yama caldera floor.

The Higashi-yama somma, the oldest body of the volcano, has been fairly dissected due to marine erosion and exposes radial dikes cutting the volcanic body. However, other volcanic bodies, Nishi-yama and the Central cone, remain free from such intense erosion. The visible part of the volcano probably ranges from late Pleistocene to

Table 1 Sequence of the evolution of Oshima-Ōshima

Parasitic crater lave	Ol-Au basalt	*Historic eruptions in: 1759, 1768 & 1790*
Central cone ejecta	Ol-Au basalt	
Central cone lava	Ol-Au basalt	
Nishi-yama ejecta		Formation of caldera *1741—1742*
scoria	Ol-Au basalt	
pumice	(Au, Hy) Bi-Ho andesite	
Nishi-yama upper lava	Au-Ol basalt	Intrusion of dykes of Ol-Au basalt
Nishi-yama middle lave	(Ol) Au-Hy andesite (Hy) Ol-Au andesite Au-Hy andesite (Ol, Ho) Au-Hy andesite Ho-Au-Hy andesite Au-Hy-Ho andesite	
Nishi-yama lower lava	Au-Ol basalt Ol-Au basaltic andesite	
		Marine erosion
Higashi-yama upper lava	Au-Ol basalt (Hy) Ol-Au andesite	Formation of caldera Intrusion of dykes of Ol-Au basalt
Higashi-yama middle lava	Hy-Au-Ho andesite Ol-Au basalt	Ol andesite
Higashi-yama lower lava	Au-Ol basalt (Hy) Au-Ol andesite (Hy) Ol-Au-Ho andesite	

Katsui et al. (1979).

Holocene in age.

The basement rocks of the volcano are not exposed anywhere. It can be inferred, however, that they are Paleozoic sediments and Mesozoic plutonic rocks which are similar to those developed in the southwestern part of Hokkaido, judging from xenoliths found in the volcanic products.

The sequence of development of the volcano is shown in Table 1. In the early stage, alternate eruptions of andesite and basalt took place from Higashi-yama (the Higashi-yama lower lava). Andesite eruptions continued (the Higashi-yama middle lava), followed by eruptions of basalt (the Higashi-yama upper lava). During the growth of this gigantic stratovolcano, built up of basalt and andesite, intrusions of radial dikes of basalt (Hd) took place. The subsidence of the summit of the stratovolcano resulted in formation of a caldera which is now surrounded by the Higashi-yama somma on the east.

During a long period of quiescence the volcanic edifice of Higashi-yama was subjected to marine erosion. Basalt and andesite were then erupted within the caldera of Higashi-yama to form the second stratovolcano which completely covered the western part of the caldera. This second stratovolcano is called Nishi-yama volcano. Eruptions of basalt took place in the early stage of Hishi-yama (Nishi-yama lower lava).

Andesites were erupted later to form lava banks and a lava delta (Nishi-yama middle lava). This activity was followed by eruptions of picritic basalt (Nishi-yama upper lava) which covered the southern part of Nishi-yama volcano. During the growth of the Nishi-yama stratovolcano, radial dikes of basalt (Nd) also intruded the volcanic edifice. Following a violent eruption that successively produced augite- and hypersthene-bearing biotite hornblende andesite pumice, then scoria, and finally olivine augite basalt bombs (Nishi-yama ejecta), the top of Nishi-yama stratovolcano collapsed to form another caldera to the north. This successive eruption occurred in 1741 after about 1,500 years of dormancy (Katsui et al., 1977; Katsui and Yamamoto, 1981). According to recent studies by Hatori and Katayama (1977) and Katsui and Yamamoto (1981), the sector collapse of Nishi-yama was triggered by a great earthquake ($M \geq 7.5$) which possibly occurred in the sea bottom near Oshima-Ōshima and generated a destructive tsunami during the culminating phase of the 1741 eruption.

The 1741 eruption continued to the next year, and a Central cone of basaltic tephras and lavas (Cl) was built within the horseshoe-shaped caldera. Flank eruptions also occurred at points on the northwestern and northeastern foot of the Central cone. Aa lavas of basalt were extruded from small craters opened at both points. After the intense eruption in 1741-1742, the activity of the Central cone decreased substantially and ceased in 1790.

Ptrography

Volcanic rocks

The rock types recognized in Oshima-Ōshima Volcano are shown in Table 1. All of the lavas and pyroclastics of the Central cone consist of olivine-augite basalt, whereas those of Nishi-yama and Higashi-yama are composed of basalt and andesite which are intimately associated with each other, even within a single cycle of eruption as in the recorded eruption in 1741-1742 (Table 1). The basalt and andesite from Oshima-Ōshima show generally porphyritic or plagiophyric texture. The typical rock types found in each volcanic edifice are as follows.

Higashi-yama somma

Higashi-yama lower lava (Hl)

*Hypersthene-bearing olivine-augite-hornblende andesite (VI d)**

The phenocrysts consists of abundant plagioclase, amphibole, clinopyroxene, olivine, iron-titanium oxide, orthopyroxene and rare apatite. Plagioclase shows remarkably oscillatory zoning and has dusty inclusions. Amphibole is strongly opacitized and includes olivine with resorption rims of iron oxide in places. Olivine is anhedral and is usually rimmed with iddingsite and iron oxide, which is further surrounded with amphibole or fine grained pyroxene in places. Clinopyroxene shows zoning and hour-glass structure, and is rarely fringed with orthopyroxene. The ground-

* The type of ferromagnesian silicate mineral assemblage by Kuno (1954).

mass shows hyalopilitic texture and consists of abundant glass, plagioclase, iron-titanium oxide, clinopyroxene, orthopyroxene, and cristobalite. Cristaobalite occurs in vesicles or inner part of honey-combed plagioclase phenocrysts.

Higashi-yama middle lava (Hm)

Biotite-bearing hypersthene-augite-hornblende andesite (VI d)

The phenocrysts are composed of abundant plagioclase, amphibole, clinopyroxene, orthopyroxene, iron-titanium oxide, and accessory mica and apatite. Oscillatory zoning and dusty inclusions are conspicuous in plagioclase. Amphibole is completely opacitized or rimmed by iron-titanium oxide. Other mafic phenocrysts are fine grained. Iron-titanium oxide (titanomagnetite) usually contains exsolution lamellae of magnetite and ilmenite. Olivine is anhedral and shows kink banding in some specimens. The groundmass shows hyalopilitic or cryptocrystalline texture and consists of plagioclase, anhedral anorthoclase, clinopyroxene, orthopyroxene, amphibole, reddish opacitized amphibole, iron-titanium oxide and glass. Fine-grained tridymite is rarely recognized in vesicles.

Higashi-yama upper lava (Hu)

Augite-olivine basalt (IV b)

The phenocrysts consist of plagioclase, olivine and clinopyroxene. Plagioclase is usually more abundant than mafic phenocrysts and is glass- or dust-charged. The groundmass shows intergranular-intersertal texture and consists of abundant prismatic plagioclase, anorthoclase, fine grained clinopyroxene and olivine, and iron-titanium oxide. Tiny crystals of chromite are included in olivine phenocrysts. There are no silica minerals in the groundmass. A small amount of interstitial glass is also recognized.

Higashi-yama dike (Hd)

Olivine-augite basalt (IV b)

About 50 vol. % of the phenocrysts are plagioclase and the rest is clinopyroxene and olivine. This rock is characterized by the presence of abundant clinopyroxene. Groundmass texture is intergranular at the center of the dike and intersertal with vesicles at the margin and consists of abundant plagioclase (about 50 vol. %), clinopyroxene, irontitanium oxide, olivine, and glass.

Nishi-yama somma

Nishi-yama lower lava (Nl)

1. Augite-olivine basalt (IV b)

Plagioclase, olivine and clinopyroxene are the essential phenocryst minerals. In addition to small chromite grains which are included in olivine phenocrysts, there are a few large chromite phenocrysts thinly rimmed with titanomagnetite. The groundmass shows intergranular texture and consists of plagioclase, clinopyroxene, olivine, anorthoclase and iron oxide. No silica minerals are found in the groundmass.

2. Olivine-augite basaltic andesite (IV b)

The upper part of the Nishi-yama lower lava consists mainly of this rock type, which occurs characteristically as thick lava flows (2-10 m), and shows plagiophyric texture. The color index is slightly lower than the basalt, being 11.5 in phenocrysts and 35.1 in groundmass. The type of ferromagnesian silicate mineral assemblage (kuno, 1954) is IV b. This rock type is recognized as a more differentiated alkali basalt.

Plagioclase, clinopyroxene and olivine are essential phenocryst minerals. Plagioclase is generally large and includes small amounts of anhedral clinopyroxenes, iron-titanium oxides and glass. Clinopyroxene shows zoning and hour-glass structure. Minor phenocrystal olivine is also observed. The groundmass shows intergranular texture and consists of plagioclase, clinopyroxene, olivine, iron-titanium oxide and anorthoclase. No silica minerals are found.

Nishi-yama middle lava (Nm)

1. Hypersthene-bearing olivine-augite andesite (Vd)

About 80 vol. % of the phenocrysts are plagioclase and the rest are clinopyroxene, olivine, orthopyroxene and rare iron-titanium oxide. Plagioclase is clear and nearly homogeneous for the most part, except oscillatory zoned margins. Clinopyroxenes show zoning and include small amounts of tiny grains of plagioclase, orthopyroxene and iron-titanium oxide. Orthopyroxene occurs as normal phenocrysts and as fine grained reaction rims around anhedral olivine. Olivine is mostly anhedral and is rimmed by orthopyroxene grains. The groundmass shows hyalopilitic texture, comprising glass, plagioclase, orthopyroxene, clinopyroxene and iron-titanium oxide. As olivine disappears in reaction with liquid, orthopyroxene increases in volume and becomes equal to clinopyroxene in the groundmass. Tridymite and cristobalite are found in vesicles.

2. Hornblende- and olivine-bearing augite-hypersthene andesite (VI d)

Plagioclase, orthopyroxene and clinopyroxene are essential phenocryst minerals. Plagioclase is more abundant than mafic phenocrysts and shows conspicuous zoning. Orthopyroxene is more abundant than clinopyroxene. Olivine is usually corroded and in places displays kink banding. Amphibole is highly corroded and surrounded by opacite rims or crystal clots of discrete grains of pyroxene, plagioclase and iron-titanium oxide. Both olivine and amphibole phenocrysts are considered as separated crystals from ultramafic and mafic inclusions which occur abundantly in this andesite lava ("Nampa-Misaki lava"). Iron-titanium oxide is present as an accessory mineral. The groundmass shows pilotaxitic — hyalopilitic texture, and consists of plagioclase, clinopyroxene, orthopyroxene, iron-titanium oxide, glass, and cristobalite.

3. Augite-hornblende-hypersthene andesite (VI d)

The phenocrysts consist of plagioclase, orthopyroxene, amphibole, clinopyroxene, iron-titanium oxide and rare apatite. About 70 vol. % of the phenocrysts are plagioclase that shows oscillatory zoning. Clinopyroxene also shows zoning and includes tiny

grains of plagioclase and glass. amphibole is abundant compared with other Nishi-yama middle lavas, and is rimmed by iron-titanium oxide. Iron-titanium oxide (titano-magnetite) generally has exsolution lamellae of magnetite and ilmenite. The ground-mass shows hyalopilitic texture and consists of plagioclase, iron-titanium oxide, glass, orthopyroxene and clinopyroxene.

Nishi-yama upper lava (Nu)

Augite-olivine basalt (IV b)

About 50 vol. % of the phenocrysts are olivine followed in order of abundance by clinopyroxene, plagioclase and rare chromite. This basalt of the Nishi-yama upper lava is the most olivine-rich of the volcanic rocks of Oshima-Ōshima, and is almost equivalent to picritic basalt. Plagioclase shows zoning and has many glass and dust-inclusions. Clinopyroxene shows zoning and no pleochroism. There are a few large chromite phenocrysts thinly rimmed with titanomagnetite, in addition to small chromite grains which are included in olivine phenocrysts. The groundmass consists of plagioclase, clinopyroxene, olivine, iron-titanium oxide, anorthoclase and glass, and shows intersertal — intergranular texture.

Nishi-yama ejecta (Ne)

During the 1741-1742 activity the composition of the volcanic rocks changed from calc-alkaline hornblende andesite to silica-undersaturated olivine-augite basalt.

1. Augite- and hypersthene-bearing biotite-hornblende andesite (pumice)

The lower layer of the Nishi-yama ejecta is made up of andesitic pumice, which is generally less than 5 cm and rarely up to 30 cm in size. Bread-crust bombs and less vesdiculated pumice are also included in the lower layer. Phenocrystic minerals are small in size and consist of plagioclase, amphibole, mica, orthopyroxene, clinopyro-xene and iron-titanium oxide. The groundmass consists of colorless clear glass which is vesiculated in various degrees.

2. Augite-olivine basaltic scoria (IV b)

The scoria is also vesiculated and shows porphyritic texture. The phenocrysts con-sist of plagioclase, olivine, clinopyroxene and rare chromite. Plagioclase is generally more abundant than mafic minerals. Chromite occurs both as large crystals thinly rim-med with iron-titanium oxide and as tiny grains included in olivine phenocrysts. The groundmass shows intersertal texture and is made up of vesiculated brown glass, plagioclase, clinopyroxene, olivine and rare iron-titanium oxide.

Central cone

Central cone lava (Cl)

Olivine-augite basalt (IV b)

Plagioclase, clinopyroxene and olivine are essential phenocryst minerals.

Plagioclase shows conspicuous oscillatory zoning and has dusty inclusions. Clinopyroxene also shows marked zoning. Clusters of olivine, clinopyroxene, amphibole, plagioclase and rare iron-titanium oxide, are found in this basalt in places, resulting in glomeroporphyritic textures. Amphibole megacrysts are rarely found. The groundmass shows intergranular — intersertal texture and consists of plagioclase, clinopyroxene, olivine, iron-titanium oxide and interstitial brown glass.

Parasitic crater lava (Cp)

Olivine-augite basalt (IV b)

The phenocrysts consist of plagioclase, clinopyroxene and olivine. About 50 vol. % of the phenocrysts are plagioclase. The groundmass shows intersertal texture and consists of abundant plagioclase, anorthoclase, and finegrained clinopyroxene, olivine and iron-titanium oxide.

Ultramafic and mafic inclusions

(1) Mode of occurrence

Ultramafic and mafic inclusions from Oshima-Ōshima Island occur abundantly in andesite lavas of the Higashi-yama middle lava and the Nishi-yama middle lava, and in andesitic pumice of the Nishi-yama ejecta. The size of these inclusions ranges from 5 mm to 40 cm in diameter. These inclusions are concentrated in the basal part of the Nishi-yama middle lava ("Nampa-misaki lava"). Isolated crystals derived from these inclusion masses are scattered along the flow structure in the host lavas. Distortion of the flow laminae is found around the inclusions in the lava where the adjacent laminae were crumpled by rotation of the inclusions. Most of the inclusions are rounded except the dunite inclusions which are usually small in size (>3 cm) and angular in shape. In these andesitic lavas and ejecta, accidental lithic fragments of the basement rocks (paleozoic sediments and plutonic rocks) are also found.

(2) Classification and nomenclature

Based upon their modal compositions, the inclusions are classified into following types: dunite, wehrlite, olivine-clinopyroxenite, clinopyroxenite, hornblendite, and hornblende gabbro (Text-figs. 3 and 4). Anorthosite, gabbro and hornblende-clinopyroxene rock are rarely found. The frequency of occurrence of these inclusions is shown in Text-fig. 5.

(3) Microscopic features

Dunite

Dunite shows olivine adcumulate texture (Wager et al., 1960). Olivine and rare clinopyroxene occur as cumulus phases. In the space between the cumulus olivine grains and clinopyroxene, a small amount of olivine and amphibole occur as an intercumulus phase. Large crystals of spinel are formed between the grain boundaries of olivine and clinopyroxene, and small euhedral crystals are also included in the olivine.

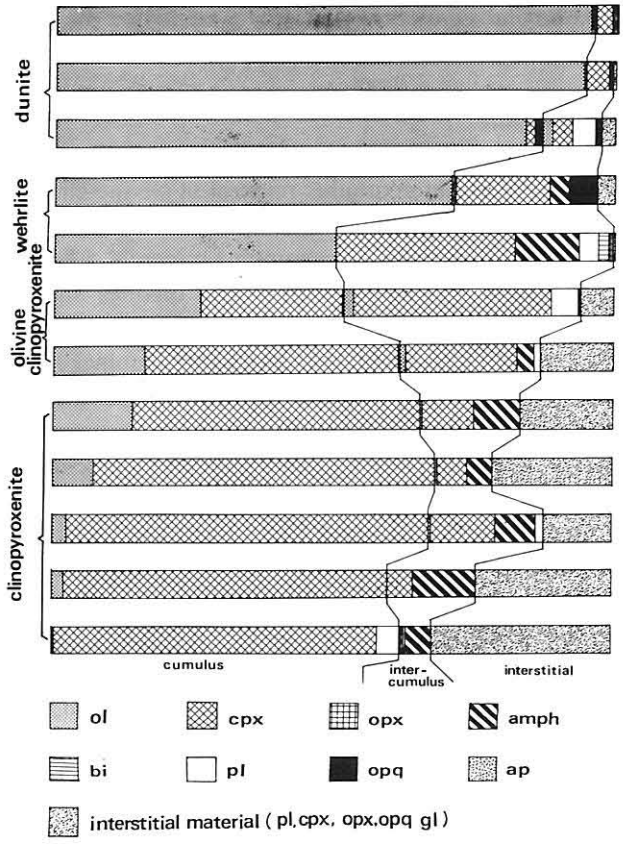

Text-fig. 3 Modal compositions of the ultramafic inclusions from Oshima-Ōshima.
ol: olivine, cpx: clinopyroxene, opx: orthopyroxene, amph: amphibole, bi: biotite, pl: plagioclase, opq: opaque mineral, ap: apatite, and gl: glass.

The constituent minerals of the dunite inclusions are virtually unzoned, homogeneous, and fresh. Other characteristic features of the dunite inclusions are 1) a very small amount of interstitial material consisting of quenched plagioclase, pyroxene and brown glass found along grain boundaries between cumulus or intercumulus phase and 2) kink banding in the cumulate olivine crystals.

Wehrlite

Wehrlite shows olivine meso- and orthocumulate texture. Most of olivines, rare clinopyroxene and spinel are recognized as a cumulus phase. The cumulus olivine has no kink banding, which is a different feature from that of the dunite. The intercumulus phase consists of olivine, clinopyroxene, amphibole, plagioclase, orthopyroxene, spinel, and rare mica. The intercumulus olivine and clinopyroxene are more abundant than those in the dunite, and they surround poikilitically or ophitically the cumulus olivine. Amphibole margins are resorbed and fine grains of iron-titanium oxide are produced there. There are some amphiboles which are included as patches in clinopyroxene. The volume of these intercumulus minerals is large compared with that of the dunite, and reaches nearly 50%. The interstitial materials, which consists of brown

glass, tiny grains of iron-titaniuim oxide, and slender crystals of pyroxene and plagioclase, also increase in volume.

Olivine-clinopyroxenite and clinopyroxenite

It is a characteristic feature that clinopyroxene appears as a cumulus mineral, whereas a small amount of olvine occurs as an intercumulus mineral in olivine-clinopyroxenite and clionpyroxenite. These rocks show olivine-clinopyroxene orthocumulate texture. Clinopyroxene, olivine and rare spinel are cumulus minerals. Clinopyroxenes in the clinopyroxenites are large in size (2-3 mm), and olivines small (1-0.5 mm) relative to their sizes in dunites. The total amount of intercumulus minerals, which consist of clinopyroxene, olivine, amphibole, plagioclase, spinel and rare orthopyroxene, is larger in olivine clinopyroxenite than in clinopyroxenite. These minerals surround poikilitically the cumulus olivine and pyroxene. The intercumulus clinopyroxene has conspicuous cleavage and zoning compared to the cumulus clinopyroxene. Amphibole is generally rimmed with opacite. Rare orthopyroxenes are found at the margins of olivines as reaction rims. Plagioclase is usually calcic ($>An_{90}$) and has a narrow labradorite rim ($=An_{50}$) ("lower temperature zone": Wager et al., 1960). Acicular plagioclase of labradorite composition has grown from the Ab-rich rim. Slender Plagioclase of labradorite composition occurs in the interstitial space together with brown glass and pyroxene. It is a characteristic feature that the constituent minerals are loosely gathered and the amount of the interstitial material is larger in the clinopyroxenite than in the olivine-clinopyroxenite.

There are some varieties of clinopyroxenite, though not so abundant, whose tex-

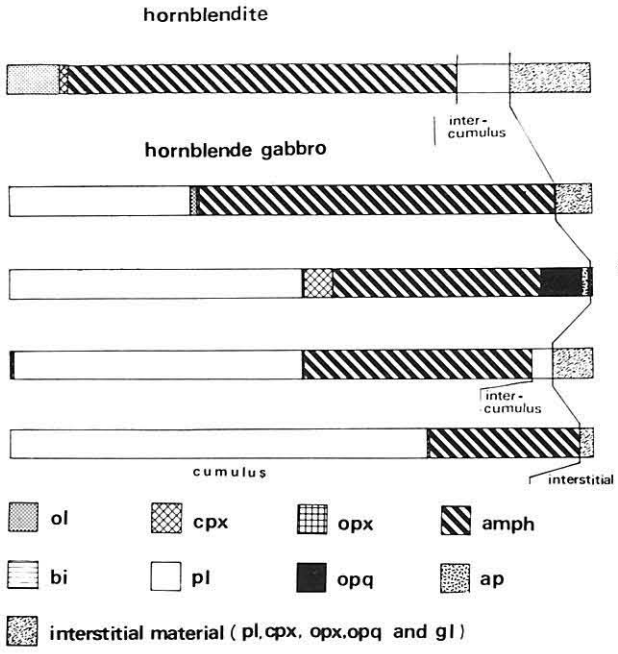

Text-fig. 4 Modal compositions of the mafic inclusions from Oshima-Oshima.
ol: olivine, cpx: clinopyroxene, opx: orthopyroxene, amph: amphibole, bi: biotite, pl: plagioclase, opq: opaque mineral, ap: apatite, and gl: glass.

tural and mineralogical features are similar to those mentioned above. One is olivine-hronblende-clinopyroxenite which carries more abundant cumulus olivine and intercumulus amphibole. The other is olivine-clinopyroxene-hornblende gabbro, in which cumulus plagioclase appears.

Gabbro

Both plagioclase and clinopyroxene are the essential minerals of the gabbro. This rock shows plagioclase-orthocumulate texture. Cumulus minerals consist of plagioclase, olivine and spinel. Intercumulus minerals consist of clinopyroxene, olivine with orthopyroxene reaction rims, mica and iron-titanium oxide. Interstitial material is composed of only brown glass.

This rock is rarely found and is considered as a transitional type from clinopyroxenite to hornblende gabbro.

Hornblendite

The constituent minerals of cumulus and intercumulus phases are loosely gathered in the interstitial materials which consist of brown glass, lath-like plagioclase, acicular

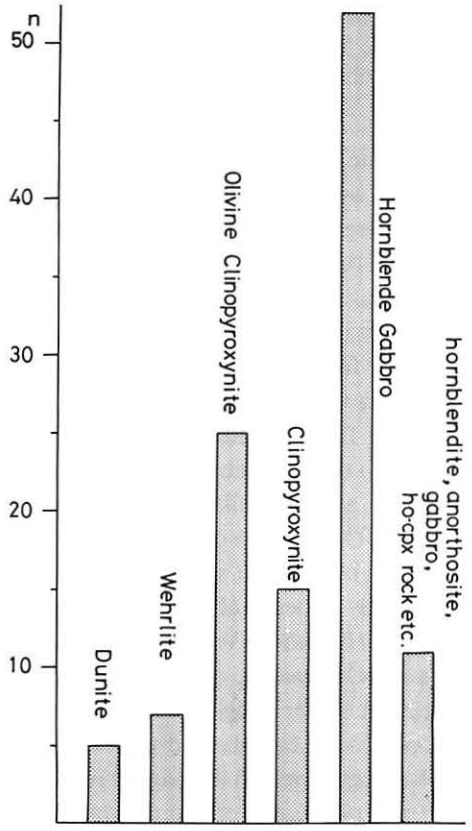

Text-fig. 5 Numbers of ultramafic and mafic inclusions found in the Nishi-yama middle lava at the coast of Aidomari, Oshima-Ōshima.

pyroxene and fine-grained iron-titanium oxide. Cumulus olivine and clinopyroxene are poikilitically or ophitically surrounded by large cumulus amphibole. The olivine is corroded and rimmed with iron-titanium oxide. The clinopyroxene is also corroded and is in places replaced by patches of amphibole. The amphibole occurs as large euhedral crystals surrounded partly by interstitial material and partly by intercumulus plagioclase. The intercumulus mineral is entirely calcic plagioclase ($>An_{90}$), which is clear and virtually unzoned except for a thin outer rim of labradorite.

Hornblende gabbro

Hornblende gabbro is the most abundant of the inclusions from Oshima-Ōshima. Plagioclase and amphibole are essential minerals of the rock whose texture resembles "plagioclase heteradcumulate" (Wager et al., 1960). The amphibole occurs as an intercumulus phase, but is virtually unzoned. Accordingly, the amphibole is considered to be a "heterad material" (Wager et al., 1960). The amphibole is rimmed with opacite. The plagioclase is euhedral and rarely shows zoning at the margin. The intercumulus minerals consist of olivine, clinopyroxene, orthopyroxene, apatite and iron-titanium oxide. The intercumulus olivine is corroded and is rimmed with iron-titanium oxide, amphibole and orthopyroxene. The clinopyroxene is also corroded and is surrounded or replaced by amphibole.

Major and trace element chemistry of the volcanic rocks

Major elements

Chemical analyses and CIPW norms of the volcanic rocks from Oshima-Ōshima are listed in Table 2 together with those reported by Katsui and Satoh (1970).

Kuno (1960) showed a zonal distribution of the three basalt types (alkali olivine basalt, high-alumina basalt and tholeiite) which are distinguished from each other by their alkali contents. It is a characteristic feature that the rocks from the Chōkai Volcanic Zone, which comprises Oshima-Ōshima and many other volcanoes along the Japan Sea coast, are richer in alkali contents than those from the Nasu Volcanic Zone.

The alkali-silica relation of the rocks from Oshima-Ōshima and other volcanoes belonging to the Chōkai Volcanic Zone is shown in Text-fig. 6. Oshima-Ōshima basalts ($SiO<53\%$) belong to the alkali rock series according to the classification by the ferromagnesian silicate mineral assemblage (Kuno, 1954) and the alkali-silica diagram (Kuno, 1966) (Text-fig. 6.). All andesites from Oshima-Ōshima are classified into "d" type of the hypersthenic rock series (Kuno, 1954) which is regarded as the calc-alkaline rock series. The rocks from Oshima-Ōshima are generally richer in alkalis, especially in potassium content, than those from other volcanoes of th Chōkai Volcanic Zone. It is noteworthy that both basalt and andesite from Oshima-Ōshima are distinguished from those from other volcanoes of the Chōkai Volcanic Zone by their higher alkali contents (Text-figs. 6 and 7). It is concluded that the alkali olivine basalts and calc-alkaline andesites from Oshima-Ōshima have similar alkali contents, which are higher in other Quaternary volcanic rocks in Hokkaido (Katsui et al., 1978), especially in potassium.

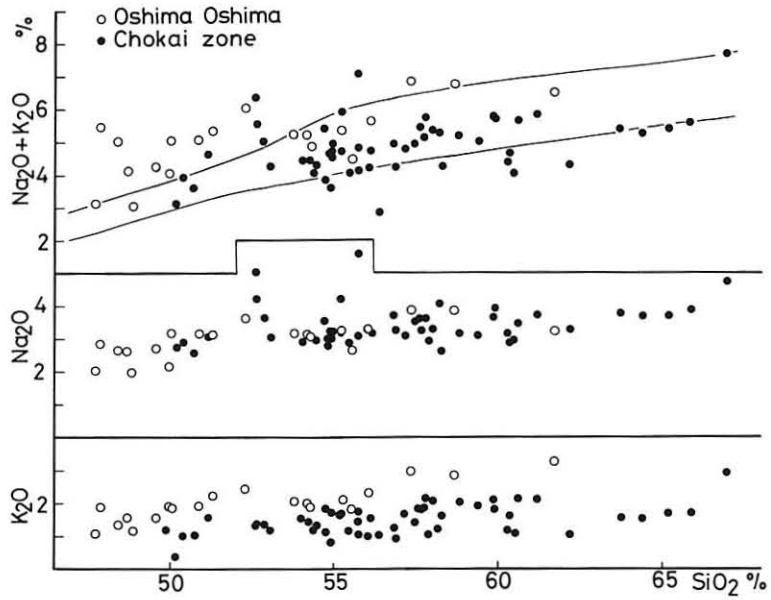

Text-fig. 6 Alkali vs. silica diagram for the rocks from Oshima-Ōshima and those from other volcanoes of the Chōkai Volcanic Zone (Data from Kawano et al., 1961; Onuma, 1963)

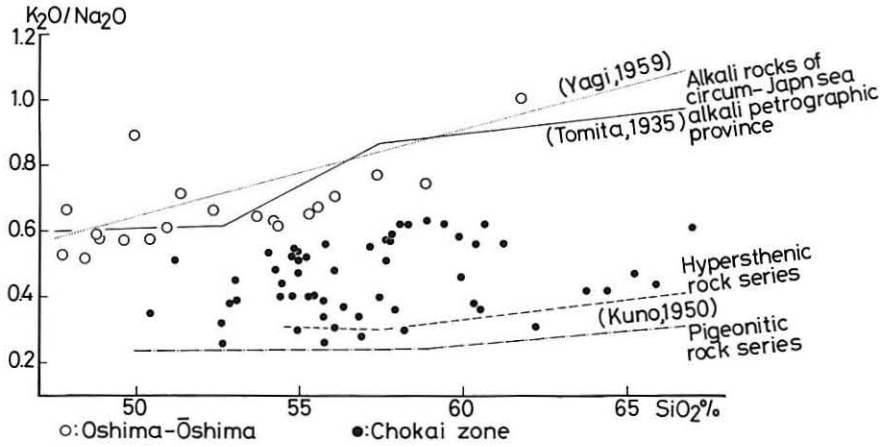

Text-fig. 7 K_2O/Na_2O vs. silica diagram for the rocks from Oshima-Ōshima and those from other volcanoes of Chōkai Volcanic Zone. The trend of principal volcanic rock series in Japan and surrounding areas are also shown (after Kuno, 1950; Tomita, 1935; Yagi, 1959).

This observation may provide an important clue in solving the genetic problem of the calc-alkaline andesite-alkali olivine basalt association at Oshima-Ōshima.

The chemical compositions are also plotted in AFM diagram (Text-fig. 8). The rocks of the Chōkai Zone are generally poor in iron contents compared with those of

Table 2 Chemical analyses and CIPW norms of Oshima-Ōshima rocks

	1	2	3	4	5	6	7	8	9	10	11	12	13	14
SiO_2	47.84	50.04	53.80	58.80	61.72	49.60	48.41	48.89	52.31	54.32	54.20	55.26	55.56	56.07
TiO_2	0.98	0.92	0.78	0.63	0.37	0.95	1.09	1.02	0.95	0.60	0.61	0.62	0.61	0.50
Al_2O_3	13.87	17.30	17.81	17.49	17.71	17.06	17.59	15.00	17.54	18.85	19.27	17.74	18.28	18.03
Fe_2O_3	6.87	2.33	4.30	3.58	1.12	2.36	3.93	2.92	4.83	4.06	2.36	3.21	2.46	4.09
FeO	4.87	5.78	4.99	2.91	4.33	6.88	7.00	6.41	5.02	3.81	4.88	4.57	5.11	3.53
MnO	0.15	0.07	0.19	0.10	0.10	0.09	0.15	0.25	0.10	0.13	0.17	0.18	0.19	0.18
MgO	9.03	8.32	3.67	2.69	1.83	5.96	5.O8	10.60	4.03	3.67	4.78	3.96	4.05	3.88
CaO	10.32	9.68	8.69	0.66	5.19	11.05	12.21	10.91	8.42	9.00	9.02	8.44	8.57	8.23
Na_2O	2.83	3.19	3.18	3.85	3.21	2.70	2.65	1.95	3.63	3.02	3.18	3.24	2.67	3.29
K_2O	1.88	1.84	2.04	2.86	3.28	1.54	1.37	1.13	2.40	1.87	2.02	2.11	1.80	2.32
H_2O (+)	1.20	0.80	1.52	0.79	0.83	0.45	n.d.	0.64	0.25	0.60	n.d.	0.46	0.62	0.50
H_2O (−)	0.69	0.27	0.30	0.07	0.16	0.13	0.16	0.12	0.08	0.01	0.09	0.02	0.13	0.13
P_2O_5	0.36	0.42	0.42	0.34	0.20	0.42	0.25	0.05	0.53	0.46	0.50	0.46	0.22	0.37
Total	100.89	100.96	101.69	100.77	100.05	99.19	99.89	99.89	100.09	100.40	101.08	100.27	100.27	101.12
Q	—	—	5.05	9.31	14.11	—	—	—	0.72	6.73	2.28	5.89	8.29	6.79
Or	11.13	11.13	12.24	16.70	19.48	8.90	8.35	6.68	13.91	11.13	11.69	12.24	10.57	13.91
Ab	22.02	24.31	26.74	32.51	27.26	23.07	21.30	16.78	30.93	25.69	26.74	27.26	22.54	27.79
An	19.47	27.54	28.37	22.25	24.20	29.76	31.99	28.65	24.48	32.26	32.54	27.81	32.54	27.54
Ne	1.14	1.31	—	—	—	—	0.67	—	—	—	—	—	—	—
Di Wo	12.19	7.55	5.11	3.83	0.35	9.41	11.27	10.57	5.81	4.06	3.72	4.76	3.48	4.53
Di En	9.84	5.17	3.21	2.81	0.10	5.52	6.63	7.43	3.91	2.91	2.31	2.91	2.01	3.21
Di Fs	0.92	1.78	1.58	0.66	0.26	3.43	4.09	2.24	1.45	0.79	1.19	1.58	1.32	0.92
Hy En	—	—	5.92	3.91	4.42	2.91	—	7.33	6.12	6.22	9.64	6.93	8.03	6.42
Hy Fs	—	—	3.03	0.92	6.20	1.85	—	2.24	2.37	1.85	5.01	3.56	5.41	1.71
Ol Fo	8.86	10.87	—	—	—	4.50	4.22	8.16	—	—	—	—	—	—
Ol Fa	0.81	4.08	—	—	—	3.06	2.75	2.85	—	—	—	—	—	—
Mt	9.96	3.47	6.25	5.09	1.62	3.47	5.79	4.17	6.95	5.79	3.47	4.63	3.47	6.02
Il	1.82	1.82	1.52	1.21	0.76	1.01	2.12	1.97	1.82	1.21	1.21	1.21	0.21	1.91
Ap	1.01	1.01	1.01	0.67	0.34	1.82	0.67	0.13	1.35	1.01	1.35	1.01	0.67	1.01

the Nasu Zone.

A Harker diagram of the Oshima-Ōshima rocks is shown in Text-fig. 9. It is noted that in their major element chemistry almost continuous variation curves can be traced from the basalt to andesite without any notable break. It is also noticed that the trend of MgO content changes considerably from the basalt to andesite. The basalt decreases rapidly in MgO content from about 15 to 5 wt%, whereas the andesite decreases gradually in MgO. The FeO/MgO ratio of the andesite is characteristically low. The olivine of high Fo contents forming the upper mantle can not be equilibriated with such andesitic magma, which suggests that the andesitic magma has not been derived through partial melting of mantle material. The trends of Al_2O_3 and alkali contents

Table 2 continued

		15	16	17	18	19	20
SiO_2		47.75	48.71	51.33	57.35	49.90	50.92
TiO_2		0.79	0.99	0.91	0.53	1.09	0.93
Al_2O_3		13.26	16.16	17.66	17.45	16.05	18.26
Fe_2O_3		3.01	6.09	4.16	2.90	5.03	1.89
FeO		6.57	4.18	5.03	3.48	5.55	5.79
MnO		0.08	0.13	0.08	0.05	0.14	0.12
MgO		15.13	8.78	5.05	2.58	7.03	5.53
CaO		9.70	11.06	9.80	6.99	10.51	9.98
Na_2O		2.04	2.60	3.10	3.88	2.15	3.13
K_2O		1.07	1.54	2.22	2.99	1.92	1.91
H_2O (+)		0.64	0.78	0.39	1.50	0.26	0.56
H_2O (−)		0.02	0.01	0.10	0.24	0.06	0.06
P_2O_5		0.31	0.38	0.57	0.42	0.23	0.42
Total		100.37	101.42	100.40	100.36	99.92	99.50
Q		—	—	—	6.19	0.66	—
Or		6.12	8.90	13.36	17.81	11.13	11.13
Ab		17.30	22.02	26.21	33.03	18.35	26.21
An		23.92	28.09	27.54	21.14	28.37	30.32
Ne		—	—	—	—	—	—
Di	Wo	9.41	10.10	7.43	4.99	9.18	6.97
	En	6.93	8.33	5.02	3.21	6.63	4.22
	Fs	1.58	0.53	1.85	1.45	1.71	2.37
Hy	En	3.21	3.11	5.92	3.21	10.84	3.11
	Fs	0.66	0.26	2.11	1.58	2.64	1.71
Ol	Fo	19.26	7.32	1.13	—	—	4.50
	Fa	4.69	0.41	0.40	—	—	2.85
	Mt	4.40	8.80	6.02	4.17	7.41	2.78
	Il	1.52	1.82	1.67	1.06	2.12	1.82
	Ap	0.67	1.01	1.35	1.01	0.67	1.01

1. Ol-Au basalt (Higashi-yama lower lava) (Hl-72)
2. (Ol)-Au basalt (Higashi-yama lower lava) (H1-76)
3. (Ol)-andesite (Higashi-yama lower lava) (H1-73)
4. Ho-Au-Hy andesite (Higashi-yama middle lava) (Hm-44)
5. Ho-Au-Hy andesite (Higashi-yama middle lava) (H-21)
6. Ol-Au basalt (Higashi-yama upper lava) (Hu-100)
7. Ol-Au basalt (Higashi-yama dyke) (Hd-49)
8. Au-Ol basalt (Nishi-yama lower lava) (H-18)
9. Al-Au basaltic andesite (Nishi-yama lower lava) (N1-14)
10. (Ol)-Au-Hy andesite (Nishi-yama middle lava) (Nm-46)
11. (Ho)-Au-Hy andesite (Nishi-yama middle lava) (Nm-107)
12. (Ho)-Au-Hy andesite (Nishi-yama middle lava) (Nm-108)
13. (Ol, Ho)-Au-Hy andesite (Nishi-yama middle lava) (H-20)
14. Hy-Au-Ho andesite (Nishi-yama middle lava) (Nm-63)
15. Au-Ol basalt (Nishi-yama upper lava) (Nu-104)
16. Ol-Au basalt (Nishi-yama ejecta, scoria) (Ne-56)
17. Ol-Au-Ho basaltic andesite (Nishi-yama ejecta, scoria) (Ne-56)
18. (Hy, Au) Bi-Ho andesite (Nishi-yama ejecta, pumice) (Ne-11)
19. Ol-Au basalt (Parsitic crater lava) (H-19)
20. Ol-Au basalt (Central cone lava) (C1-119)

Analyses 5, 8, 13 & 19 (Katsui and Satoh, 1970)

also change notably. The content of Al_2O_3 increases abruptly in the basalt, whereas it becomes almost constant or decreases slightly in the andesite. The alkali content increases slightly in the basalt, whereas between $SiO_2 = 51$-56 wt% it remains nearly constant, increasing slightly thereafter. The different oxide variation trends in the basalts and andesites may have resulted from the different crystallization sequences in each rock suite.

Trace elements

The concentration of three trace elements, Rb, Ba and Sr, was determined by atomic absorption spectrophotometry by means of the method developed by

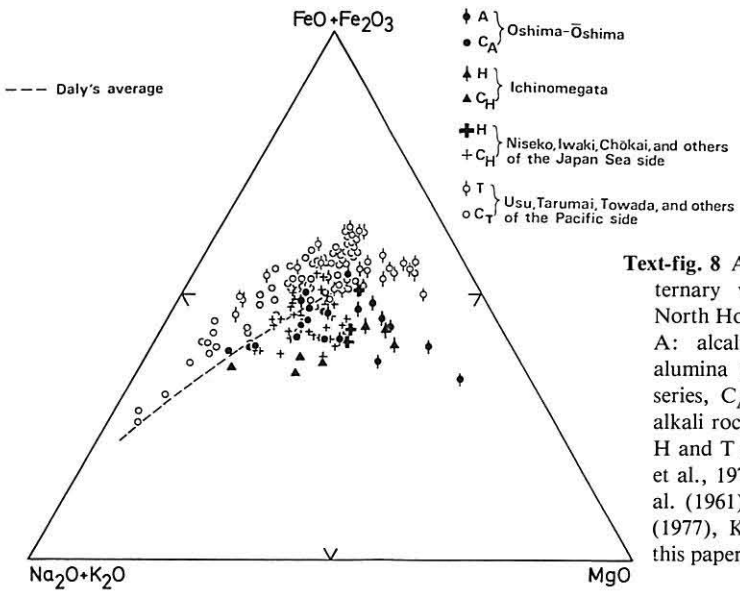

Text-fig. 8 AFM diagram for the Quaternary volcanic rocks from the North Honshū Arc, northern Japan. A: alcali rock series, H: high-alumina basalt series, T: tholeiite series, C_A, C_H and C_T and calc-alkali rock series associated with A, H and T series, respectively (Katsui et al., 1978). Data from Kawano et al. (1961), Ōnuma (1963), Togashi (1977), Katsui et al. (1977, 1978), this paper and unpublished analyses.

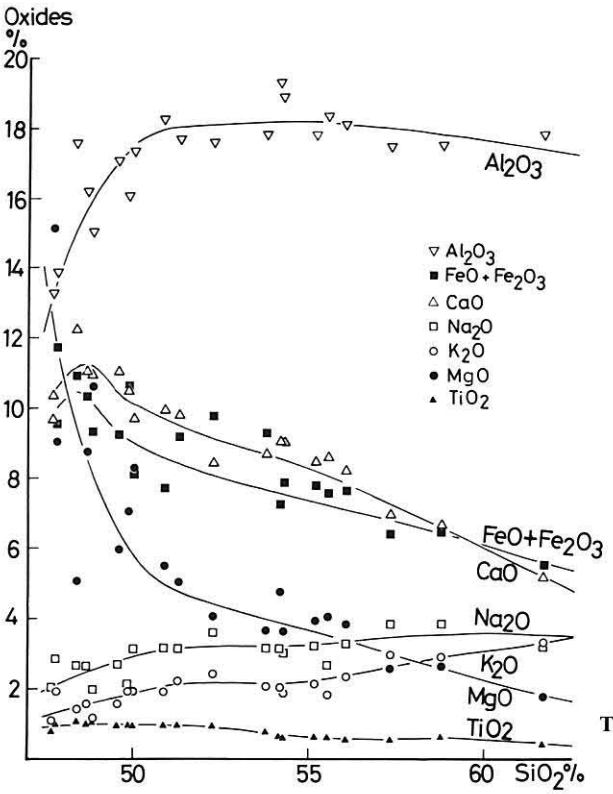

Text-fig. 9 Harker diagram for the rocks from Oshima-Ōshima.

Terashima (1971, 1973). The analytical data are listed in Table 3. Chemical composition of major and rare-earth elements in four H_{18}, H_{19}, H_{20} and H_{21} were reported by Katsui and Satoh (1970) and Masuda et al. (1975), respectively. The normalized rare-earth patterns of rare-earth elements (REE patterns) for the basalts (H_{18} & H_{19}) and the andesites (H_{20} & H_{21}) are shown in Text-fig. 10, respectively. It is noticed that lighter REE are enriched from H_{18} (SiO_2 48.89 wt%) to H_{19} (SiO_2 49.90%). No Eu anomaly is shown in the basalts, whereas the andesites (H_{20}:SiO_2 55.56 wt%, H_{21}: SiO_2 61.72 wt%) have an obvious Eu anomaly. These data reflect the different crystalliza-

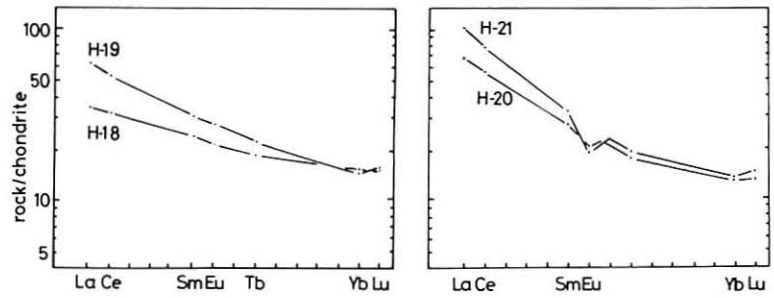

Text-fig. 10 Chondrite-normalized rare-earch elements pattern (Masuda et al., 1975).

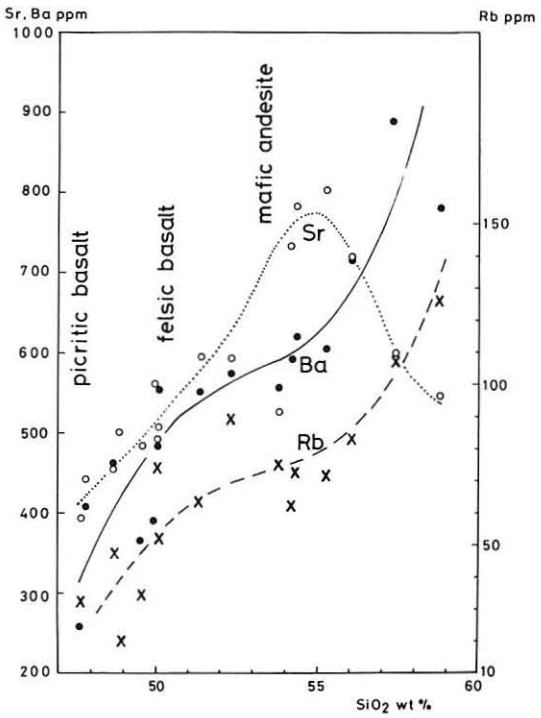

Text-fig. 11 Trends of Rb, Ba and Sr in the Oshima-Ōshima volcanic rocks.

tion sequence between the basaltic and andesitic magmas in Oshima-Ōshima volcano.

Rb, Ba and Sr vs. silica diagrams for 15 rocks from Oshima-Ōshima are shown in Text-fig. 11. The trends of Rb and Ba concentrations resemble those of the alkali contents as mentioned above. The Sr concentration abruptly increases from the basalt to mafic andesite (SiO_2 55 wt%), then decreases with an increase in SiO_2.

Table 3 Analytical data for trace elements.
All values in ppm except SiO_2

	sp.no.	SiO_2%	Rb	Ba	Sr
1	Nu-104	47.75	32	256	394
2	Hl-72	47.84	72	407	441
3	Ne-56	48.71	47	462	455
4	Hu-100	49.60	33	366	482
5	Hl-76	50.04	51	480	493
6	Cl-119	50.92	74	551	506
7	Ne-54	51.33	63	552	595
8	Nl-14	52.31	89	575	593
9	Hl-73	53.80	75	556	526
10	Nm-107	54.20	62	591	734
11	Nm-46	54.32	72	619	781
12	Nm-108	55.26	71	606	803
13	Nm-63	56.07	82	713	720
14	Ne-11	57.35	107	889	598
15	Hm-44	58.80	126	779	546

Petrogenesis

Most of the andesite and rare basalt contain ultramafic and mafic inclusions such as dunite, wehrlite, olivine-clinopyroxenite, clinopyroxenite, hornblendite and hornblende gabbro which typically show cumulus texture. For the petrognesis of the calc-alkaline andesite of Oshima-Ōshima, it is important to determine whether these inclusions were formed as cognate cumulates in the basaltic and andesitic magma, or not.

Crystallization of the ultramafic and mafic inclusions

All of the inclusions show cumulate textures as already mentioned. The following features of the inclusions are noticed with regard to their origin.

(1) In Oshima-Ōshima island, hornblende gabbro is most abundant followed by clinopyroxenite and its varieties and wehrlite in order of abundance. Occurrence of dunite is relatively rare.

(2) The dunite inclusions are small in size and angular in shape. They are occasionally surrounded by clinopyroxenite and hornblende gabbro, but not vice versa. Kink bands are found in the olivines of dunite, but not in those of other inclusions.

(3) Olivine gradually decreases and clinopyroxene gradually increases in modal

abundance in the order dunite, wehrlite, olivine-clinopyroxenite, clinopyroxenite (Text-fig. 3).

(4) Modal compositions of intercumulus minerals in the dunite and wehrlite become similar to whole modal compositions of the clinopyroxenite.

(5) The cumulus olivine decreases in amount from the dunite to clinopyroxenite, and the intercumulus olivine is present in small amounts in all inclusion types. The cumulus clinopyroxene increases in amount from the wehrlite to clinopyroxenite.

(6) The amount of interstitial material increases gradually from the dunite to clinopyroxenite.

(7) The cumulus olivine and clinopyroxene are more abundant in hornblendite than in hornblende gabbro. The amphibole in the hornblendite is obviously cumulus, whereas that in the hornblende gabbro is considered to be a heterad material (Wager et al., 1960). The plagioclase in the hornblendite is intercumulus, whereas that in hornblende gabbro is obviously cumulus.

Chemical analyses of olivine, clinopyroxene and amphibole are listed in Tables 4, 5 and 6. Mg/Mg+Fe ratios of these minerals decrease as follow: dunite → wehrlite → clinopyroxenite → hornblende gabbro (Text-fig. 12).

Obata et al. (1974) pointed out that Mg-Fe partitioning between olivine and clinopyroxene can be used as an empirical geothermometer. The data of the inclusions indicate that olivine and clinopyroxene were equilibrated at a temperature near 1000°C (Text-fig. 13). Therefore, the ultramafic and mafic inclusions are considered to be the products crystallized from basaltic magma. The crystallization sequence of these inclusions is suggested as follows: dunite → wehrlite → olivine-clinopyroxenite → clinopyroxenite → hornblendite → hornblende gabbro. It is inferred that the dunite formed at a deeper level than the others, based on its occurrence. The pressure conditions of crystallization of these inclusions will be discussed later.

Chemical characteristics of the magma which crystallized the ultramafic and mafic inclusions

Since the inclusions from Oshima-Ōshima were probably equilibrated at high temperatures, it is likely that they were not derived from the continental crust, but were formed by crystallization of basaltic magma. The petrographical features of these inclusions suggest that they are cognate cumulates associated with the volcanic rocks of Oshima-Ōshima.

Amphiboles in the inclusions from Oshima-Ōshima are classified into pargasite and pargasitic hornblende by plotting Si and Ca + Na + K (Leake, 1968). These amphiboles are plotted in this diagram together with those from various other locations (Text-fig. 14). The amphiboles associated with felsic rocks are generally enriched in Si content and classified as common hornblende. Si values of the amphiboles from granitic rocks (Kanisawa, 1972, 1975 and 1976) and dacitic rock (Nicholls, 1971) exceed 6.50.

In Text-fig. 14, the amphiboles from the Oshima-Ōshima inclusions are pargasitic in composition and are similar to others from basanitoid and basalt from the Lesser

Table 4 Selected microprobe analyses of olivines from the inclusions

Sp.no.	1 RS22-3	2 RS22-2	3 725-2	4 725-4	5 RS5-2	6 RS3-2	7 RS102-12	8 RS102-5	9 RS20-2	10 730-7-3′	11 730-7-7′	12 730-7-5
SiO_2	40.27	39.79	40.29	40.17	39.31	39.06	41.40	37.91	38.50	37.47	38.55	38.52
TiO_2	0.00	0.00	—	—	0.01	0.06	—	—	0.02	—	—	—
Al_2O_3	0.01	0.02	0.01	0.01	0.00	0.02	0.00	0.01	0.04	0.02	0.02	0.00
FeO	9.07	9.13	12.90	13.51	18.31	19.46	19.43	21.81	19.82	21.16	22.81	22.85
MnO	0.11	0.17	0.18	0.23	0.33	0.31	0.32	0.40	0.39	0.93	0.46	0.54
MgO	49.98	50.34	46.02	45.95	42.12	41.12	40.09	39.10	40.44	39.49	38.52	38.55
NiO	—	—	0.22	0.28	—	—	0.30	0.15	—	—	—	—
CaO	0.09	0.10	0.13	0.09	0.09	0.06	0.14	0.14	0.11	0.11	0.10	0.14
Na_2O	0.00	0.03	—	—	0.01	0.00	—	—	0.00	—	—	—
K_2O	0.00	0.00	—	—	0.00	0.01	—	—	0.00	—	—	—
Total	99.53	99.58	99.75	100.24	100.18	100.10	101.68	99.38	99.32	99.18	100.49	100.61
Numbers of cations on the basis of 4 oxygens												
Si	0.989	0.979	1.004	1.000	1.001	1.035	0.991	0.997	0.983	1.001	0.999	
Al	0.001	0.001	0.000	0.000	0.000	0.001	0.000	0.000	0.001	0.001	0.001	0.000
Ti	0.000	0.000	—	—	0.000	0.001	—	—	0.000	—	—	—
Fe	0.186	0.188	0.269	0.281	0.390	0.417	0.406	0.477	0.430	0.464	0.495	0.496
Mn	0.002	0.004	0.004	0.005	0.007	0.007	0.007	0.009	0.009	0.021	0.010	0.012
Mg	1.830	1.846	1.710	1.705	1.598	1.570	1.508	1.524	1.562	1.545	1.490	1.491
Ni	—	—	0.004	0.006	—	—	0.006	0.003	—	—	—	—
Ca	0.003	0.003	0.003	0.002	0.003	0.002	0.004	0.004	0.003	0.003	0.003	0.004
Na	0.000	0.002	—	—	0.001	0.000	—	—	0.000	—	—	—
K	0.000	0.000	—	—	0.000	0.000	—	—	0.000	—	—	—
Total	3.011	3.011	2.994	2.999	2.999	2.998	2.966	3.008	3.002	3.017	3.000	3.002
$\frac{100 \times Mg}{Mg+Fe+Mn}$	90.7	90.6	86.2	85.6	80.1	78.7	78.5	75.8	78.1	76.1	74.7	74.6

1-4: dunite, 5-8: wehrlite, and 9-12: clinopyroxenite
(1-2, 5-6, 9: analyst K. Niida)
Microprobe analyses were carried out using the electron microprobe, JSM-50A at Governemnt Industrial Development Laboratory, Hokkaido and JXA-5A at Geological Survey of Japan and the correction was made by the method of Bence and Albee (1968) and by the method of Sweatman and Long (1969), respectively.

Table 5 Selected microprobe analyses of clinopyroxenes from the inclusions

Sp.no.	1 RS22-7	2 725-3	3 725-6	4 RS3-1	5 RS20-5	6 RS20-9	7 RS6-10	8 RS6-9	9 RS6-6	10 730-9-5	11 730-9-5	12 730-9-(5)
SiO_2	52.97	52.43	51.83	51.30	50.85	50.43	51.28	50.63	51.11	52.32	50.60	51.55
TiO_2	0.31	0.37	0.58	0.74	0.48	0.76	0.60	0.56	0.64	0.35	0.62	0.43
Al_2O_3	2.46	3.60	4.88	4.19	3.82	4.39	3.96	4.33	4.25	1.80	3.38	2.48
Cr_2O_3	—	0.70	0.69	—	—	—	—	—	—	—	—	—
FeO	2.56	4.39	4.24	5.33	5.39	5.63	5.72	6.01	6.15	7.67	8.61	10.25
MnO	0.07	0.09	0.18	0.06	0.10	0.08	0.16	0.15	0.12	0.48	0.43	0.31
MgO	17.19	15.86	15.56	15.12	14.76	15.64	15.57	15.53	16.17	14.82	16.30	—
CaO	23.90	22.37	22.65	22.87	24.10	23.88	22.77	22.75	22.72	20.41	20.58	16.76
Na_2O	0.26	0.25	0.32	0.24	0.15	0.15	0.23	0.28	0.24	0.23	0.28	0.29
K_2O	0.02	—	—	0.00	0.00	0.01	0.00	0.00	0.00	0.01	0.02	0.02
Total	99.74	100.07	100.92	99.79	100.11	100.09	100.36	100.28	100.76	99.44	99.34	98.39
Numbers of cations on the basis of 6 oxygens												
Si	1.933	1.916	1.880	1.891	1.879	1.865	1.884	1.886	1.874	1.946	1.986	1.939
Al^{IV}	0.067	0.084	0.120	0.110	0.121	0.135	0.116	0.134	0.126	0.054	0.104	0.061
Al^{VI}	0.039	0.071	0.089	0.073	0.046	0.056	0.056	0.055	0.057	0.025	0.046	0.049
Ti	0.008	0.010	0.016	0.021	0.014	0.021	0.017	0.016	0.018	0.010	0.018	0.012
Cr	—	0.020	0.020	—	—	—	—	—	—	—	—	—
Fe	0.078	0.134	0.129	0.164	0.170	0.174	0.176	0.185	0.189	0.239	0.270	0.323
Mn	0.002	0.003	0.006	0.002	0.003	0.003	0.005	0.005	0.004	0.015	0.014	0.010
Mg	0.935	0.864	0.841	0.827	0.833	0.813	0.857	0.855	0.849	0.896	0.828	0.914
Ca	0.934	0.876	0.880	0.903	0.955	0.946	0.896	0.899	0.893	0.813	0.827	0.676
Na	0.019	0.018	0.023	0.017	0.011	0.011	0.016	0.020	0.017	0.017	0.020	0.021
K	0.001	—	—	0.000	0.000	0.000	0.000	0.000	0.000	0.001	0.001	0.001
Total	4.016	3.996	3.981	4.006	4.030	4.024	4.022	4.034	4.026	4.014	4.022	4.005
Ca	48.0	46.7	47.9	47.6	48.7	48.9	46.5	46.3	46.3	41.4	42.7	35.2
Mg	48.0	46.0	45.3	43.7	42.6	42.1	44.4	44.1	43.9	45.6	42.7	47.5
Fe+Mn	4.0	7.3	7.3	8.7	8.7	9.0	9.1	9.6	9.8	12.9	14.6	17.3
$\frac{100\times Mg}{Mg+Fe+Mn}$	92.1	86.3	86.2	83.4	82.8	82.2	82.6	81.8	81.5	77.9	74.5	73.3

1-3: dunite, 4-6: wehrlite, 7-9: clinopyroxenite, 10-12: hornblende gabbro

Table 6 Selected microprobe analyses of amphiboles from the inclusions

Sp.no.	1 725-6	2 725-5	3 725-1	4 RS3-3	5 RS3-6	6 RS3-10	7 RS6-2	8 RS20-6	9 RS6-3	10 730-9-9	11 730-9-10	12 730-9-8
SiO_2	42.76	43.99	41.92	44.12	43.28	42.64	42.72	41.55	41.98	42.09	41.77	41.82
TiO_2	1.63	1.31	2.17	2.24	2.50	2.68	1.86	1.72	2.00	1.88	1.74	2.09
Al_2O_3	11.87	12.37	13.05	10.90	11.97	12.20	12.96	13.77	13.84	13.43	13.58	13.24
Cr_2O_3	1.37	1.19	1.32	—	—	—	—	—	—	—	—	—
FeO	6.17	6.71	6.34	8.74	8.98	9.14	9.48	9.53	9.86	9.80	9.91	9.94
MnO	0.14	0.09	0.07	0.11	0.09	0.10	0.13	0.12	0.13	0.11	0.14	0.09
MgO	16.67	17.42	16.27	16.64	15.76	15.25	15.64	15.21	14.88	15.36	15.38	15.33
CaO	12.11	11.69	12.44	11.55	11.87	12.03	11.78	12.62	11.86	11.76	11.57	11.95
Na_2O	2.32	2.17	2.35	2.21	2.16	2.30	2.31	2.07	2.14	2.04	2.15	1.95
K_2O	0.85	1.01	1.06	0.87	1.02	1.15	0.82	1.10	1.13	1.02	1.08	1.05
Total	95.89	97.95	96.99	97.38	97.63	97.49	97.70	97.69	97.82	97.49	97.32	97.46
Numbers of cations on the basis of 23 oxygens												
Si	6.285	6.317	6.116	6.416	6.298	6.239	6.224	6.087	6.131	6.159	6.132	6.134
Al^{IV}	1.715	1.683	1.884	1.584	1.702	1.761	1.777	1.913	1.869	1.841	1.869	1.866
Al^{VI}	0.341	0.411	0.360	0.286	0.352	0.344	0.449	0.465	0.514	0.476	0.482	0.424
Ti	0.180	0.141	0.238	0.245	0.274	0.294	0.204	0.189	0.220	0.207	0.193	0.231
Cr	0.159	0.135	0.152	—	—	—	—	—	—	—	—	—
Fe	0.758	0.806	0.774	1.062	1.094	1.119	1.155	1.167	1.205	1.199	1.217	1.220
Mn	0.017	0.011	0.009	0.013	0.012	0.013	0.016	0.015	0.016	0.014	0.018	0.011
Mg	3.653	3.729	3.539	3.606	3.418	3.326	3.395	3.320	3.239	3.351	3.365	3.352
Ca	1.907	1.799	1.945	1.799	1.851	1.886	1.839	1.981	1.856	0.845	0.820	1.878
Na	0.661	0.604	0.665	0.624	0.611	0.652	0.653	0.589	0.606	0.579	0.613	0.556
K	0.159	0.185	0.197	0.161	0.189	0.214	0.153	0.205	0.210	0.191	0.203	0.197
Total	15.835	15.821	15.879	15.797	15.801	15.847	15.863	15.932	15.862	15.912	15.869	
Ca	30.1	28.4	31.0	27.8	29.0	29.7	28.7	30.6	29.4	28.8	28.3	29.1
Mg	57.7	58.8	56.5	55.8	53.8	52.6	53.3	51.2	51.5	52.3	52.4	51.9
Fe+Mn	12.2	12.9	12.5	16.4	17.2	17.7	18.0	18.2	19.1	18.9	19.3	19.0
$\frac{100\times Mg}{Mg+Fe+Mn}$	82.5	82.0	81.9	77.0	75.6	74.6	74.3	73.7	72.6	73.4	73.2	73.1

1-3: dunite, 4-6: wehrlite, 7-9: clinopyroxenite, 10-12: hornblende gabbro

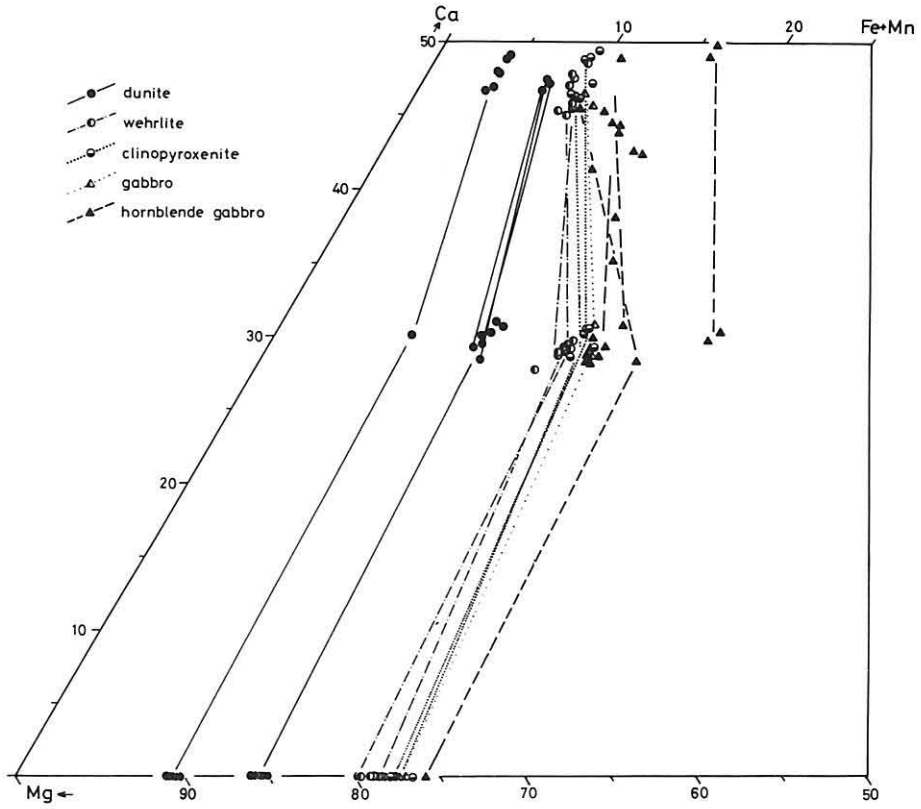

Text-fig. 12 Ca-Mg-Fe plot of clinopyroxenes, amphiboles and olivines (Ca free) from ultramafic and mafic inclusions. Tie-lines indicate minerals coexist each other.

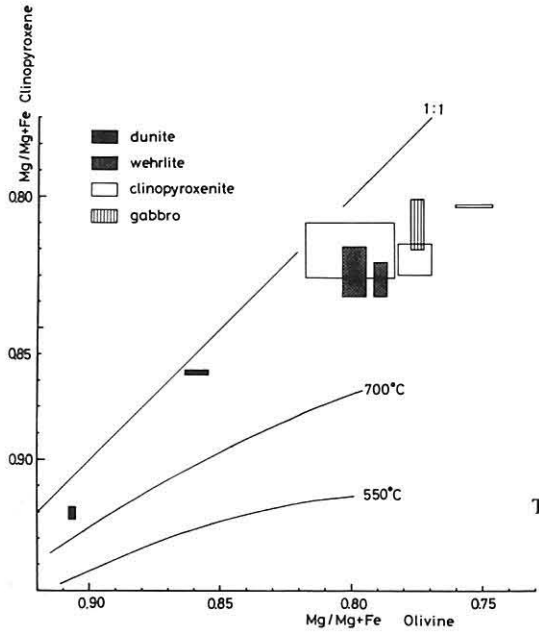

Text-fig. 13 Mg-Fe partition between olivine and clinopyroxene from the ultramafic and inclusions. Ranges in Mg/Mg+Fe are indicated.

Antilles (Cawthorn et al., 1973; Lewis 1973 a, b; Sigurdsson and Shepherd, 1974), basalt from Yoneyama (Sato et al. 1975) and basic andesite from Shigarami & Kujiranami (Yamazaki et al., 1966) and Hakusan (Tiba, 1976). In the Lesser Antilles, such Si-poor amphiboles are considered to have crystallized from basaltic magma at a relatively higher temperature (Cawthorn et al., 1973; Lewis, 1973 a, b; Sigurdsson and Shepherd, 1974). This conclusion is supported by water saturated melting experiments of natural basalts (Heltz, 1973; Cawthorn et al., 1973).

Potassium occupies the A site in amphibole and it ranges in content in the amphiboles associated with mafic volcanic rocks. The amphiboles from Oshima-Ōshima are relatively high in potassium content. In Oshima-Ōshima, as mentioned earlier, both alkali basalt and calc-alkaline andesite are high in alkali content, especially in potas-

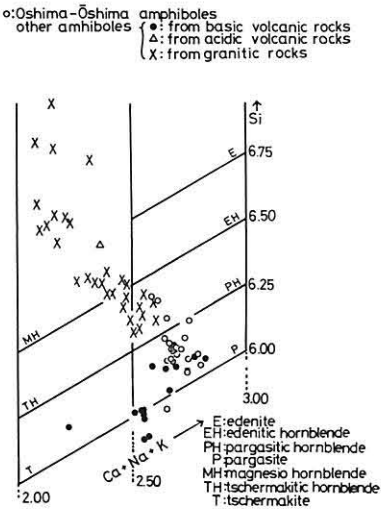

Text-fig. 14 Plot of Si and Ca + Na + K for amphiboles from Oshima-Ōshima and others. The basic volcanic rocks; basanitoid and basalt from Lesser Antilles (Cawthorn et al., 1973; Lewis, 1973 a,b; Sigurdsson and Shepherd, 1974), basalt from Yoneyama (Sato et al., 1975) and basic andesite from Sigarami & Kujiranami (Yamazaki et al., 1966) and Hakusan (Tiba, 1976). The acidic volcanic rock; dacite from Santorini (Nicholls, 1971). The granitic rocks from Japan (Kanisawa, 1972, 1975 and 1976).

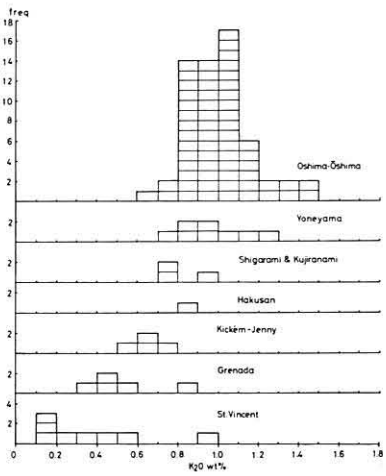

Text-fig. 15 K_2O frequency-distribution for amphiboles associated with basic volcanic rocks.
Yoneyama: Sato et al. (1975), Sigarami & Kujiranami: Yamazaki et al. (1966), Hakusan: Tibe (1976), Kick'em-Jenny: Sigurdsson and Shepherd (1974), Grenada: Cawthorn et al. (1973), St. Vincent: Lewis (1973 a, b).

sium, which distinguishes these rocks from those of other volcanoes of the Chōkai Volcanic Zone. The chemical character of the Oshima-Ōshima rocks is consistent with that of the amphiboles. K_2O frequency-distribution for amphiboles from mafic volcanic rocks is shown in Text-fig. 15. Amphiboles from Oshima-Ōshima, Yoneyama, Shigarami and Kujiranami are higher in K_2O contents than the others, consistent with the potassic nature of their host rocks (Sato et al., 1975; Yamazaki et al., 1966) (Text-fig. 16), whereas amphiboles from St. Vincent (Lewis, 1973 a) and Kick'em-Jenny, (Sigurdsson and Shepherd, 1974), Lesser Antilles associated with potassium-poor basalts are lower in K_2O contents. Accordingly, it is suggested that K_2O contents of amphiboles are controlled by those of their host rocks. This relationship is supported by Ujike and Onuki (1976) who investigated felsic rocks, and by experimental data on basalts (Green and Ringwood, 1968; Holloway and Burnham, 1972; Cawthorn et al., 1973; Heltz, 1973; Allen et al., 1975) (Text-fig. 17). Judging from these data and PC-IR relation in amphiboles (Matsui et al., 1977; Nagasawa and Schnetzler, 1971), the partition coefficient of K in amphibole from mafic rocks is higher than that from felsic rocks.

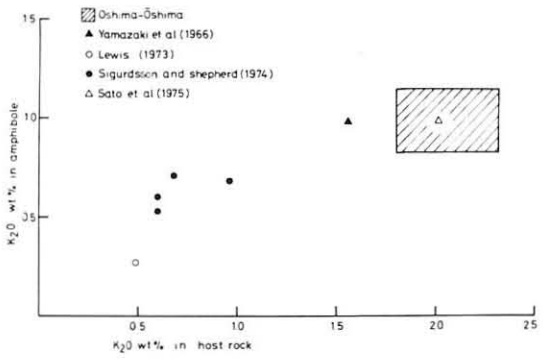

Text-fig. 16 Relation between K_2O contents in amphiboles and in host rocks. Plot of Oshima-Ōshima indicates ranges in amphiboles and rocks.

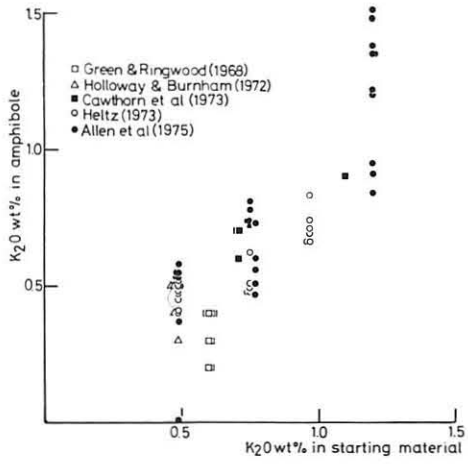

Text-fig. 17 Relation between K_2O contents of amphiboles and starting materials (natural basalts).

Therefore, it is suggested that the amphiboles of Oshima-Ōshima have crystallized from basaltic magma and they are cognate with their host volcanic rocks.

Spinels enclosed in olivines from Oshima-Ōshima show a continuous variation from chromian spinel to Fe-Ti rich spinel. Chemical analyses of spinels in basalt and ultramafic inclusions from Oshima-Ōshima are listed in Tables 7 and 8 and those in andesite from Chōkai volcano are in Table 9. Spinel generally becomes rich in magnetite component with proceeding crystallization. Since spinel can be substituted by ülvospinel, $Fe^{3+}/Cr+Al+Fe^{3+}$ ratio becomes progressively higher with increasing of Ti content through the crystallization of basaltic magma. Shiraki et al. (1979) pointed out that Ti content in spinel is controlled by that of the magma from which the spinel crystallized.

Text-fig. 18 shows various trends of the chemistry of spinels. The spinels from

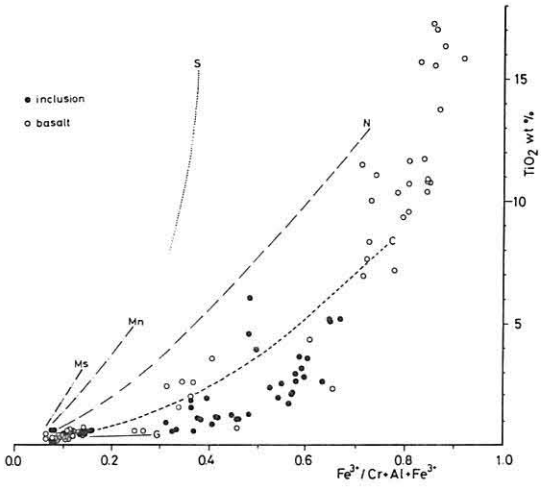

Text-fig. 18 Plot of Tio_2 wt% vs. $Fe^{3+}/Cr+Al+Fe^{3+}$ (atomic ratio) of spinels in basalt (open circle) and ultramafic inclusion (solid circle) from Oshima-Ōshima, basalt of Misasa (MS; Nagao et al., 1980), Snake River Plain basalt (S; Thompson, 1973), basanitoid of Nanzaki (N; Shiraki et al., 1979), andesite of Chōkai (C; this paper), and tholeiitic & calc-alkaline basalts of Guam (G; Shiraki et al., 1977).

Table 7 Selected microprobe analyses of the spinels in the basalts

	1	2	3	4	5	6	7	8	9	10
$TiO_2$0.25	0.54	0.55	0.51	1.58	10.34	0.58	2.01	10.71	11.64	
Al_2O_3	6.94	10.77	15.85	16.85	8.71	4.45	15.64	12.75	6.08	5.89
Cr_2O_3	56.15	48.40	42.48	40.56	33.29	3.91	32.90	26.44	0.56	0.38
Fe_2O_3	6.50	8.75	10.40	10.44	24.58	39.71	19.31	27.05	42.16	40.56
FeO	22.66	24.84	21.03	20.55	25.67	35.71	21.34	26.04	36.84	37.72
MnO	0.54	0.56	0.36	0.33	0.37	0.37	0.32	0.46	0.48	0.51
MgO	6.51	5.59	8.71	8.85	5.46	3.01	8.21	6.04	3.06	2.96
Total	99.55	99.45	99.38	98.09	99.66	97.50	98.30	100.79	99.89	99.66
$Cr/(Cr+Al)$	0.844	0.751	0.643	0.618	0.719	0.371	0.585	0.582	0.058	0.041
$Fe^{3+}/(Cr+Al+Fe^{3+})$	0.085	0.114	0.130	0.131	0.336	0.782	0.441	0.362	0.807	0.808
$Mg/(Mg+Fe^{2+})$	0.339	0.286	0.425	0.434	0.275	0.131	0.407	0.293	0.129	0.12

1-2: augite-olivine basalt (Nu-104)
3-4: olivine-augite basalt (Nu-56)
5-6: olivine-augite basalt (Hu-100)
7-8: olivine-augite basalt (Cl-119)
9-10: olivine-augite basaltic andesite (Nl-14)
Fe_2O_3 were calculated assuming stoichiometry.

Table 8 Selected microprobe analyses of the spinels in the inclusions

	1	2	3	4	5	6	7	8	9	10	11	12
$TiO_2$0.48	0.49	0.53	0.42	0.65	0.58	1.14	3.61	0.56	1.24	1.04	5.08	
Al_2O_3	28.97	27.88	30.93	26.43	17.20	15.74	19.31	11.67	12.83	15.37	13.23	10.92
Cr_2O_3	32.92	29.11	26.54	30.61	24.34	23.81	18.48	10.09	30.90	17.80	19.63	6.47
Fe_2O_3	8.93	12.08	12.25	12.43	25.72	28.55	29.87	40.53	24.96	33.83	34.70	43.23
FeO	14.38	15.72	16.11	16.68	22.65	23.96	23.85	28.44	22.92	24.29	24.46	29.00
MnO	0.18	0.29	0.27	0.19	0.29	0.27	0.32	0.27	0.43	0.39	0.34	0.37
MgO	14.75	13.30	13.70	12.66	7.53	6.73	7.66	5.05	7.03	6.74	6.33	5.59
Total	100.61	98.87	100.33	99.42	98.38	99.64	100.63	99.66	99.63	99.66	99.73	100.66
$Cr/(Cr+Al)$	0.433	0.412	0.365	0.437	0.487	0.504	0.391	0.367	0.618	0.437	0.499	0.284
$Fe^{3+}/(Cr+Al+Fe^{3+})$	0.100	0.140	0.138	0.145	0.329	0.365	0.376	0.584	0.322	0.442	0.456	0.644
$Mg/(Mg+Fe^{2+})$	0.646	0.601	0.603	0.575	0.372	0.334	0.364	0.240	0.354	0.331	0.316	0.256

1-4: dunite, 5-8: wehrlite, and 9-12: olivine-clinopyroxenite.
Fe_2O_3 were calculated assuming stoichiometry.

Table 9 Microprobe analyses of spinels from the andesites of Chōkai Volcano

	1	2	3	4	5	6
sp.no.	1C-1-1	1C-1-5	1C-1-7	1C-9-6	1C-9-5	1C-9-1
SiO_2	0.11	0.07	0.10	—	0.05	0.10
TiO_2	0.04	0.44	0.39	—	5.79	7.45
Al_2O_3	33.91	41.19	44.70	43.40	5.97	4.82
Cr_2O_3	21.01	17.83	15.11	13.56	12.76	6.56
Fe_2O_3	13.19	10.12	8.79	12.41	38.95	43.74
FeO	17.29	13.65	14.87	18.58	31.71	33.50
MnO	0.31	0.11	0.13	0.23	0.34	0.48
MgO	12.98	16.38	16.01	13.33	3.50	3.26
Total	99.20	99.79	100.10	101.51	99.07	99.91
Numbers of cations on the basis of 32 oxygens						
Si	0.026	0.016	0.022	—	0.014	0.029
Ti	0.072	0.075	0.065	—	1.261	1.624
Al	9.498	10.931	11.702	11.493	2.038	1.647
Cr	3.948	3.174	2.654	2.409	2.922	1.504
Fe^{3+}	2.360	1.715	1.470	2.099	8.492	9.545
Fe^{2+}	3.436	3.570	2.762	3.491	7.681	8.124
Mn	0.062	0.021	0.025	0.044	0.083	0.118
Mg	4.599	5.498	5.301	4.465	1.511	1.409
$\frac{100\times Mg}{Mg+Fe^{2+}}$	57.2	68.1	65.7	56.1	16.4	14.8
$Cr/Cr+Al$	0.294	0.225	0.185	0.173	0.589	0.477
$Fe^{3+}/Cr+Al+Fe^{3+}$	0.149	0.108	0.093	0.131	0.631	0.752
$Cr/Cr+Al+Fe^{3+}$	0.250	0.201	0.168	0.151	0.217	0.118
$Al/Cr+Al+Fe^{3+}$	0.601	0.691	0.739	0.718	0.152	0.113

1-3: hornblende-bearing olivine-hypersthene augite andesite
4-7: olivine-bearing hornblende-hypersthene-augite andesite
Rock samples from K. Ōnuma.

Misasa (Nagao et al., 1980), Mineoka (Tazaki, 1975) and Snake River Plain (Thompson, 1973) are high in TiO_2 wt%, whereas those from Guam (Shiraki et al., 1977) are low. The spinels from Oshima-Ōshima (Tables 7 and 8) are lower than those from Nanzaki (Shiraki et al., 1979) and are similar to those from Chōkai (Table 9). The TiO_2 content of the Oshima-Ōshima rocks less than 1 wt%, is similar to that of Chōkai volcano. It is noticed that the TiO_2 contents of spinels and their host rocks from Oshima-Ōshima and Chōkai, in the same volcanic zone, are similar to each other.

It is also noticed that the spinels in ultramafic inclusions (solid circles in Text-fig. 18) and those in basalts (open circles) from Oshima-Ōshima volcano show the same trend. This chemical feature of both spinels suggests that the ultramafic inclusions are cognate with the volcanic rocks.

The chemistry of the amphiboles and spinels which occur in the volcanic rocks and ultramafic & mafic inclusions from Oshima-Ōshima has been discussed in this section. These data suggest that the ultramafic and mafic inclusions are products of crystallization from basaltic magma and that they are cognate inclusions in the volcanic rocks. It is concluded that these inclusions are integral in the fractional crystallization of the basaltic magma of Oshima-Ōshima volcano.

Crystallization of basaltic magma

(1) Simple subtraction of ultramafic and mafic inclusions from the magma

There is considerable evidence to suggest that the ultramafic and mafic inclusions have played a significant role in the differentiation of the basaltic magma in Oshima-Ōshima volcano. The variation in chemical composition of the Oshima-Ōshima alkali basalt suite is characterized by notable decrease in MgO, increase in Al_2O_3, Na_2O and K_2O, and decrease in total iron, CaO and TiO_2, with slight increase in silica content. The chemical variation of the Oshima-Ōshima calc-alkaline andesite suite is characterized by slight decrease in MgO, minor increase in $Na_2O + K_2O$, constant or minor decrease in Al_2O_3 and decrease in total iron, CaO and TiO_2, with considerable increase in silica. These variations are shown in Text-figs. 9 and 19. Assuming that the observed chemical variation trends are mainly due to extraction of the ultramafic and mafic inclusions from the magma, a subtraction diagram is employed for analysis of the variation trends (Text-fig. 19). The principal constratints on any extraction model are, of course, the ovserved chemical variation as stated above and the composition of the extracted phases. The modal compositions of the dunite, wehrlite, olivine-clinopyroxenite hornblendite and hornblende gabbro, which are essential inclusions from Oshima-Ōshima, are given in a table in Text-fig. 19. The bulk chemical compositions of these inclusions are calculated by means of their modal compositions, and chemistry and specific gravity of the constituent menerals. The specific gravity was approximated from Deer et al. (1966) as follows; olivine: 3.3 (in dunite and wehrlite) and 3.4 (in olivine-clinopyroxenite, hornblendite and hornblende gabbro), clinopyroxene: 3.3, plagioclase: 2.75, and amphibole: 3.15. The constituent minerals of the ultramafic and mafic inclusions are virtually unzoned compared with the phenocrysts in the basalt and

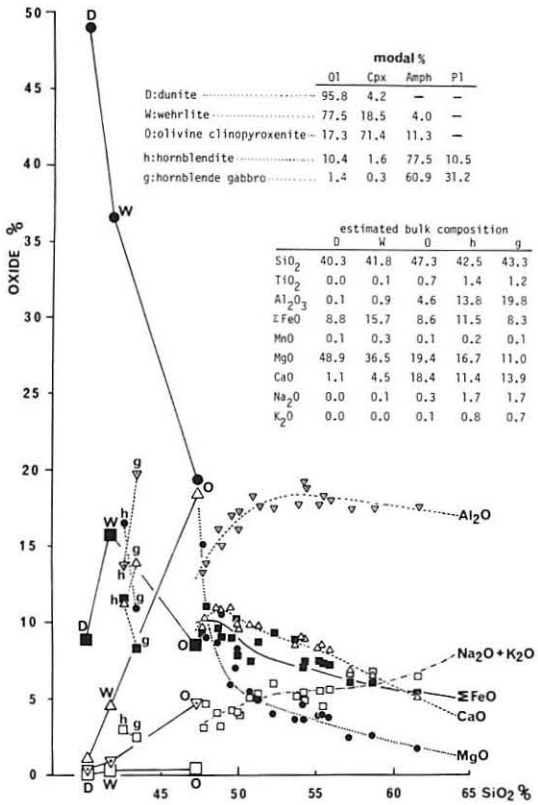

Text-fig. 19 Subtraction diagram for the Oshima-Ōshima rocks.

andesite from Oshima-Ōshima. The calculated bulk compositions of ultramafic and mafic inclusions are plotted in Text-fig. 19, together with the compositions of volcanic rocks.

The crystallization sequence of the ultramafic and mafic inclusions has been estimated as follows: dunite → wehrlite → olivine-clinopyroxenite → clinopyroxenite → hornblendite → hornblende gabbro. The MgO content of basalts abruptly decreases from picritic basalt to felsic basalt. The trend can be interpreted by removal of dunite compositions (D), which results in rapid depletion of MgO from the basaltic magma with a slight SiO_2 enrichment. Then separation of wehrlite compositions (W) and olivine-clinopyroxenite compositions (O) proceeds. Through the crystal fractionation producing dunite, wehrlite, and olivine-clinopyroxenite inclusions, the basaltic magma becomes slightly siliceous, about 51 wt.% SiO_2 and begins to produce hornblendite followed by hornblende gabbro which are lower in MgO content (16.7-11.0 wt%) than dunite, wehrlite and olivine-clinopyroxenite inclusions. Therefore, the removal of hornblendite and hornblende gabbro from the felsic basalt magma leads to a considerable enrichment of SiO_2 in the magma with a slight decrease in MgO content.

The Al_2O_3 content of basalts increases considerably from the picritic basalt to felsic basalt. Since aluminous minerals are rarely found in the dunite, wehrlite and olivine-

clinopyroxenite inclusions, the Al_2O_3 content of the basaltic magma increases with proceeding of the fractional crystallization which produces these inclusions. On the contrary, the Al_2O_3 content of the andesitic magma becomes nearly constant or decreases slightly with increasing SiO_2. Such behavior of alumina suggests the extraction of alumina-rich phases from the magma. Both amphibole and plagioclase in the inclusions are rich in Al_2O_3, being about 13 and 35 wt%, respectively. It is, therefore, suggested that the felsic basalt magma crystalized a considerable amount of hornblendite and subsequently hornblende gabbro.

The alkali content of basalts increases from the picritic basalt to felsic basalt, whereas it scarcely increases from the felsic basalt ($SiO_2 = 51\%$) to mafic andesite ($SiO_2 = 55\%$), though increasing about again in the later stages. Since alkali is a minor component in anhydrous inclusions such as dunite to olivine-clinopyroxenite, the alkali content of the basaltic magma increases with proceeding crystallization. This trend is halted, however, by crystallization of amphibole which is rich in alkali ($Na_2O = 2$ wt%, $K_2O = 1$ wt%). Microscopic observation indicates that amphibole is in a reaction relationship with olivine and clinopyroxene, which suggests that the felsic basaltic magma begins to fractionate amphibole-bearing inclusions instead of the anhydrous ultramafic ones. At the later stages of crystallization ($SiO_2 = 55\%$) the alkali content slightly increases, which suggests that the hornblende gabbro inclusions are separated from the andesitic magma, because the alkali content of the hornblende gabbro inclusion is lower than that of the magma.

The total iron and CaO contents show a slight enrichment at the earliest stage of crystallization of the basaltic magma. This trend may have been caused by the early separation of dunite inclusions from the magma. Then, both total iron and CaO decrease notably toward the most differentiated andesite, which can be interpreted as the successive removal wehrlite through hornblende gabbro compositions.

It is concluded from above examination that the ultramafic and mafic inclusions are the products of the fractional crystallization of the basaltic magma of Oshima-Ōshima volcano, and that amphibole fractionation occurred from the felsic basalt magma, which is viewed as an important factor for the evolution of the calc-alkaline andesite series in Oshima-Ōshima volcano.

(2) Rayleigh model of fractionation

Major and trace elements of two basalts (H_{18}:SiO_2 48.89%, H_{19}:49.90%) and two andesites (H_{20}:SiO_2 55.56%, H_{21}:61.72%) have been analyzed (Katsui and Satoh, 1970; Masuda et al., 1975; Katsui et al., 1978). According to earlier discussion, the four rocks are ranked in the order of differentiation as follows: $H_{18} \rightarrow H_{19} \rightarrow H_{20} \rightarrow H_{21}$. In this section, effective partition coefficients (Albarède, 1976) of various elements are determined by the method of Allègre et al. (1977) using the chemical data of these four rocks. The materials removed from the magma are then determined using the relation between the effective partition coefficients for various elements and their ionic radii (Whittaker and Muntus, 1970).

Thorium is chosen to be the H element (Allègre et al., 1977) which is used as a

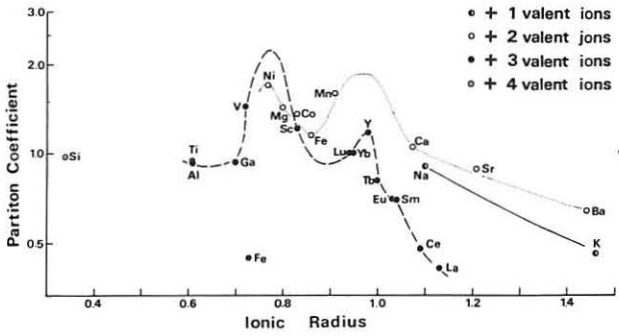

Text-fig. 20 Effective partition coefficient vs. ionic radius diagram determined by the calculation assuming Rayleigh fractionation from H_{18} to H_{19}. Ionic radii after Whittaker and Muntus (1970).

measure of the liquid fraction. The calculation of effective partition coefficient should be carried out within a narrow range of variation of element because the effective partition coefficient generally varies with composition of the mineral and the melt and also with mineral assemblage. In the case of Oshima-Ōshima, the mineral assemblages in the basaltic magma and the andesitic magma are significantly different. Therefore, separate effective partition coefficients are determined for H_{18} to H_{19} and for H_{20} to H_{21} representing the fractional crystallization of the basaltic magma and the andesitic magma, respectively.

Text-fig. 20 shows the relation between the effective partition coefficient (PC) and the ionic radii (IR) for the fractional crystallization of the basaltic magma, assuming that the initial liquid is H_{18} and residual liquid is H_{19}. The PC-IR patterns clearly show maxima at approximately 0.79Å and 1.0Å corresponding to the sites M_1 and M_2, respectively, in clinopyroxene (Jensen, 1973. data from Schnetzler and Philpotts, 1968). Text-fig. 21 shows the relation between PC and IR for the fractional crystallization of the andesitic magma, assuming that the initial liquid is H_{20} and the residual liquid is H_{21}. This PC-IR relation shows a peculiar pattern that is not correlative with any patterns which have been determined by analyses of phenocryst and matrix of natural volcanic rocks. It is noticed that the partition coefficients of Eu, Ca and Sr are considerably high. As mentioned earlier, the petrographical and mineralogical features of the inclusions, the REE pattern of the andesites, and the subtraction diagram suggeset that plagioclase played an important role in the crystallization of the andesitic magma. Therefore, this PC-IR pattern is complicated by plagioclase and another mineral which have different values of partition coefficients. This pattern may show the average value of partition coefficients of these minerals. For determination of the unknown mineral, it is necessary to remove the partition coefficients of plagioclase from this pattern. The procedure of the removal of plagioclase is as follows:

$D_{20\text{-}21}$ = the effective partition coefficients shown in Text-fig. 21.

D_{pl} = partition coefficients of plagioclase

D_x = partition coefficients of the unknown mineral Assuming that weight ratio of plagioclase and X (unknown mineral) is 1:1

$D_x = 2D_{20\text{-}21} - D_{pl}$

It is also assumed that D_{pl} is equal to the partition coefficient of the plagioclase

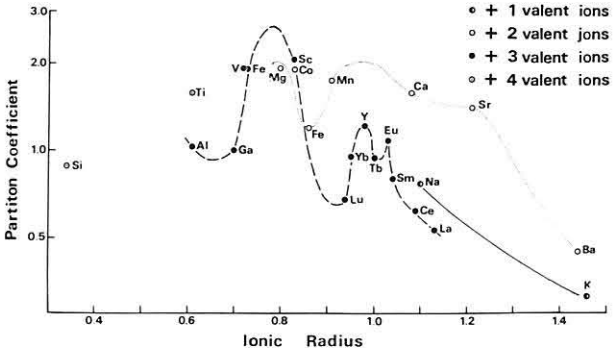

Text-fig. 21 Effective partition coefficient vs. ionic radius diagram determined by the calculation assuming Rayleigh fractionation from H_{20} to H_{21}. Ionic radii after Whittaker and Muntus (1970).

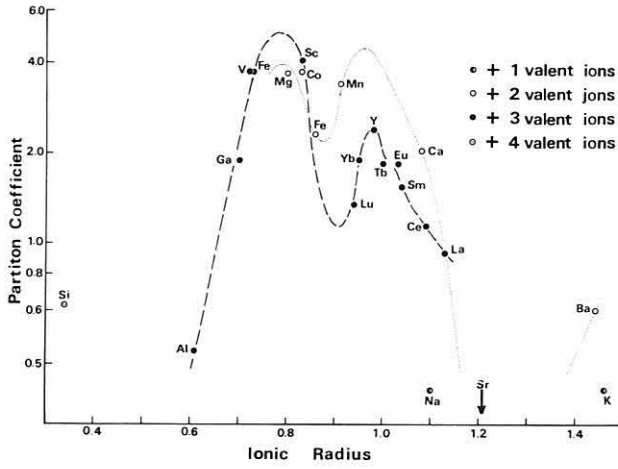

Text-fig. 22 Effective partition coefficient vs. ionic radius diagram of Dx.

from Takashima since a number of its elements are determined (Higuchi and Nagasawa, 1969). Although some partition coefficients are not determined, the missing data were estimated by the PC-IR pattern (Jensen, 1973. data from Higuchi and Nagasawa, 1969).

The resultant data from the above procedure show that the partition coefficient of Sr is close to zero, whereas that of Ba does not decrease (Text-fig. 22). The pattern of Text-fig. 22 is similar to that of amphibole which has peaks at approximately 0.78Å, 1.00Å and 1.45Å (Jensen, 1973. data from Nagasawa and Schnetzler, 1971; Matsui et al., 1977). It is a conspicuous feature that the PC-IR pattern of amphiboles has a peak at 1.45Å which suggests a large vacant site. Accordingly, the examination by the Rayleigh model shows the separation of both plagioclase and amphibole from the andesite magma, which suggests hornblende gabbro fractionation.

It is concluded from the Rayleigh model of fractionation that the clinopyroxene fractionation at the early stage and the hornblende + plagioclase fractionation at the later stage, may be important factors in the evolution of the magma in Oshima-Ōshima volcano. This conclusion is consistent with the earlier discussion.

(3) Fractionation of amphibole and plagioclase

The concentration of three elements, Rb, Ba and Sr of the volcanic rocks from Oshima-Ōshima volcano was determined by atomic absorption spectrophotometry. The features of their variation were mentioned earlier (Text-fig. 11). In Text-fig. 11, the trends of Rb and Ba concentrations resemble that of the K contents. The concentrations of Rb, Ba and K increase in the first stage from the picritic basalt to the felsic basalt, increase more gently in the second stage from the felsic basalt to the mafic andesite, and increase more steeply again in the third stage from mafic andesite. The gentle increase in Rb, Ba and K at the second stage suggests the onset of amphibole fractionation from the felsic basalt magma. This is well supported by the trends of various major elements which have been discussed in terms of the subtraction diagram (Text-fig. 19). Since Rb, Ba and K have large ionic radii, these elements tend to concentrate in amphibole, which has a large vacant site. Furthermore, the partition coefficients of these elements are higher in the amphibole associated with mafic volcanic rocks than in that associated with felsic volcanic rocks, as mentioned earlier.

The Sr concentration increases abruptly from the picritic basalt to the mafic andesite, then decreases with increase in SiO_2. Banno and Yamazaki (1979) pointed out that the Sr content has a maximum at the intermediate stage of fractionation in non-alkaline rocks, for which their model fits best. Their trend of Sr is nearly constant, whereas the trend of Sr in the Oshima-Ōshima basalt shows a steep increase. Sr is, generally, strongly concentrated into plagioclase, and the partion coefficient for Sr increases with decrease in An% ($D^{Sr} > 1$ in anorthite, >30 in oligoclase) (Jensen, 1973). The steep, positive trend of Sr in the Oshima-Ōshima basalt, therefore, suggests that the start of plagioclase fractionation is considerably delayed. This suggestion is also supported by the absence of Eu anomaly in the basalt REE pattern, but its presence in the REE pattern of the andesite, and by the subtraction diagram and Rayleigh model of fractionation, as mentioned earlier. Anorthite, which is a main constituent of the hornblende gabbro inclusions, may have a partition coefficient for Sr close to 1, but the effective partition coefficient for Sr of hornblende gabbro must be less than 1. It is, therefore, more likely that the plagioclase fractionation starts just before the magma reaches SiO_2 55%, at which point the trend of Sr peaks.

From the above discussion, it is suggested that the felsic basalt magma ($SiO_2 = 51\%$), after fractionation of anhydrous phases, crystallized amphibole to form hornblendite, and then plagioclase to form hornblende gabbro. The effective partition coefficients for K, Rb and Ba of hornblende gabbro may be lower than hornblendite because the coefficients for these elements in anorthite are quite low. The change of the effective partition coefficients is consistent with K, Rb and Ba enrichment at later stages (from SiO_2 55%).

(4) Crystallization course of the basaltic magma plotted in some phase diagrams

According to earlier discussions, it was concluded that the ultramafic and mafic inclusions have played an important role in the fractional crystallization of the magma

of Oshima-Ōshima volcano, and that their crystallization sequence is as follows; dunite → wehrlite → olivine-clinopyroxenite (associated with the differentiation from the picritic basalt magma to the felsic basalt magma), hornblendite → hornblende gabbro (associated with the differentiation from the felsic basalt magma to andesitic magma). In this section, phase diagrams will be used to trace the crystallization path of the magma in Oshima-Ōshima volcano.

A simple phase diagram for dry tholeiitic magmas at 1 atm is given in Test-fig. 23. The methods of data projection by O'Hara (1965), Cox and Hornung (1966) and Clarke (1970) are used. Phase boundaries used are quoted from Clarke (1970) and Cox and Bell (1972). The projection method is derived from CIPW norms with only minor modification. In Text-fig. 23 the fields labelled are the three-phase surface which form the boundaries of the primary phase field.

Text-fig. 23 shows that the most of the volcanic rocks from Oshima-Ōshima are plotted in the plagioclase + liquid field in accord with the plagiophyric nature of these rocks. Text-fig. 24 shows projections on the anhydrous polybaric system (O'Hara, 1968). The projection method and phase boundaries are based on O'Hara (1968). Text-fig. 24 also shows that most of the data plot in the plagioclase + liquid field at 1 atm.

Yoder (1969) pointed out that plagioclase components may be concentrated in the liquid at high pressures under anhydrous or hydrous conditions. It is therefore considered that the high aluminous residual liquid, resulting from hydrous pressure fractionation of inclusioins, became oversaturated in plagioclase under near surface conditions when the magma was ascending. Most phenocrysts characterized by the plagiophyric nature in the felsic basalt and the andesite may have originated at the very shallow place.

The concentration of plagioclase components in the rocks are controlled by the

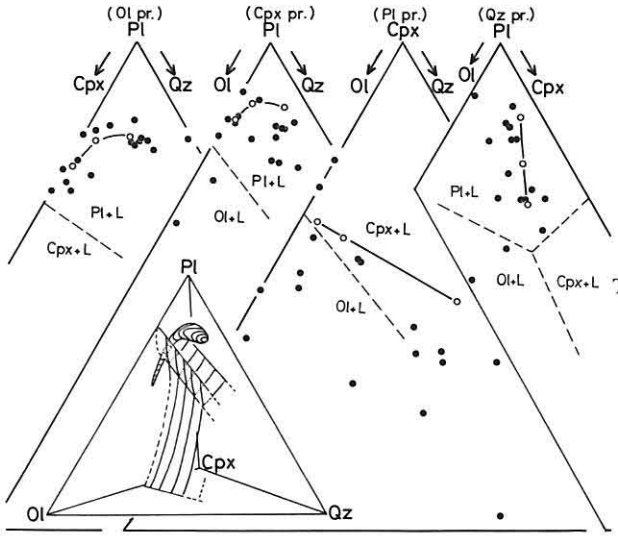

Text-fig. 23 Projection of data into the pseudo-quaternary system Ol-Cpx-Pl-Qz. Ol pr: projection from olivine, Cpx pr: projection from clinopyroxene, Pl pr: projection from plagioclase, and Qz pr: projection from quartz. The three open circles tied to each other are the pumice, felsic scoria and mafic scoria which were erupted successively in this order during 1741-1742 (Nishi-yama ejecta).

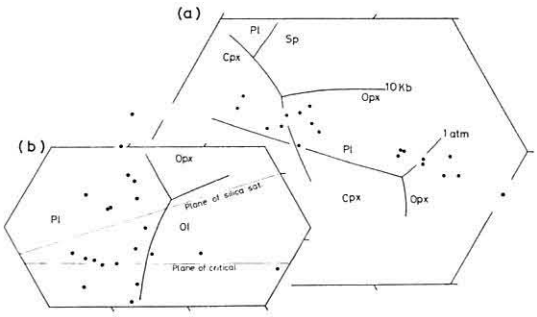

Text-fig. 24 Projection of data into phase diagram for anhydrous basalts (O'Hara, 1968).
a: projection from olivine, b: projection from diopside.

fractional crystallization of the magma of Oshima-Ōshima at higher pressures under anhydrous or hydrous conditions. Since the amphibole fractionation is considered to be an important factor in the differentiation of magma in Oshima-Ōshima volcano, the condition of the magma may be hydrous. The area occupied by the andesites plotted in Text-figs. 23 and 24 may therefore trace a cotectic line between plagioclase and amphibole under hydrous condition.

Cawthorn (1976) has studied the melting relations in part of the system CaO-MgO-Al_2O_3-SiO_2-Na_2O-H_2O under 5 kb and determined the stability of pargasitic hornblende at 5 kb in a wide range of simple basalt-like compositions. He also predicted evolution paths for water-saturated mafic magma compositions in this system. Text-fig. 25 shows the weight percent projection from diopside, vapor and Na_2O onto part

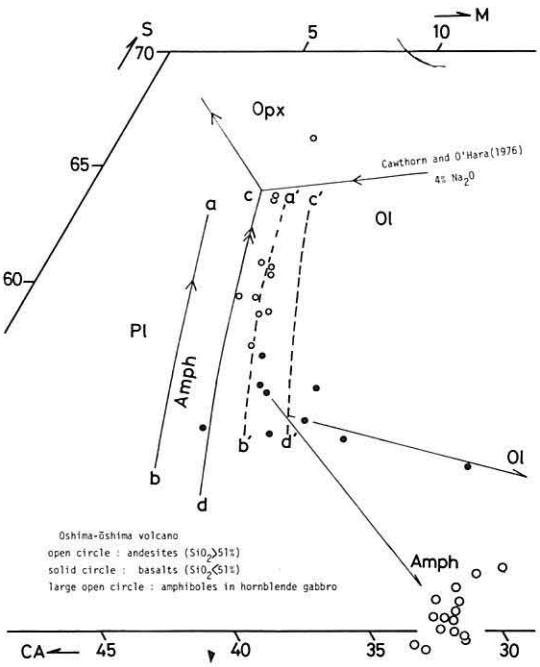

Text-fig. 25 Weight percent projection from diopside and alkali into part of the plane $CaAl_2O_4$-MgO-SiO_2 for the rocks from Oshima-Ōshima volcano.

of the plane $CaAl_2O_4$-MgO-SiO_2. The analyses of the Oshima-Ōshima volcanic rocks are calculated into components analogous to the five oxides (S: SiO_2, A: Al_2O_3, C: CaO, M: MgO, and N: Na_2O) by the method of Cawthorn and O'Hara (1976). The boundaries between the liquidus fields of olivine, amphibole, orthopyroxene and plagioclase are projected on Text-fig. 25 from diopside, Na_2O (4%) and vapor. The liquidus volume of plagioclase is reduced compared with that at anhydrous 1 atm since amphibole enters between plagioclase and olivine or clinopyroxene.

Most of chemical compositions of Oshima-Ōshima volcanic rocks plot in the olivine liquidus volume. Cawthorn (1976) and Cawthorn and O'Hara (1976) pointed out that the amphibole stability field rapidly increases with increasing Na_2O content, and both boundaries of plagioclase-amphibole and amphibole-olivine shift toward olivine liquidus volume with increasing Na_2O in the clinopyroxene projection (Text-fig. 25). The phase boundaries for $Na_2O = 6\%$ further shift from those for $Na_2O = 4\%$ toward the olivine liquidus volume. Therefore, in the case of the crystallization of Oshima-Ōshima basaltic magma which is rich in alkali, it seems that the amphibole-plagioclase cotectic line a-b and the amphibole-olivine reaction line c-d shift to a'-b' and c'-d', respectively. Accordingly, the crystallization course of the magma in Oshima-Ōshima can be considered as follows: Olivine (+clinopyroxene) crystallize first from the picritic basalt magma forcing the magma composition in the opposite direction of olivine (+clinopyroxene) to a point on the amphibole-olivine reaction line c'-d'. The olivine and clinopyroxene will react with the liquid to form amphibole.

If the magma is under "equilibrium crystallization conditions" (Cawthorn and O'Hara, 1976), its composition will change along line c'-d'. But, the plots of Oshima-Ōshima volcanic rocks suggest that the magma composition migrates across line c'-d' away from the amphibole composition, possibly due to the fractionation of olivine (+clinopyroxene) to form dunite, wehrlite and clinopyroxenite inclusions at the early stage. The felsic basalt magma then fractionates amphibole to form hornblendite, and reaches a point on the amphibole-plagioclase cotectic line a'-b'. From this point the magma will crystallize both amphibole and plagioclase to form hornblende gabbro. The fractionation of hornblendite may produce a liquid of andesitic composition. The crystallization of the magma in Oshima-Ōshima seems to have proceeded under "fractional crystallization conditions (Cawthorn and O'Hara, 1976)".

(5) Compositional variation of clinopyroxene during the crystallization

Successive removal of dunite, wehrlite and clinopyroxenite results in a considerable decrease in MgO/MgO+FeO ratio of the magma with slight SiO_2 enrichment, whereas removal of hornblendite, and hornblende gabbro leads to a slight increase in MgO/MgO+FeO ratio of the magma with a considerable SiO_2 enrichment. These variations are essential for the differentiation of the magma in Oshima-Ōshima volcano.

With proceeding crystallization, the basaltic magma is enriched in Al_2O_3, whereas the andesitic magma is only slightly enriched in Al_2O_3. This variation of Al_2O_3 is obviously caused by the delay of plagioclase crystallization under hydrous conditions.

Therefore, the Al_2O_3 trend of the Oshima-Ōshima basalt-andesite suite is important for division between the crystallization of basalt and that of andesite. Chemistry of the rock-forming minerals in the inclusions is expected to be controlled by the composition of the magma, e.g. MgO, FeO, SiO_2 and Al_2O_3 contents.

With this in mind, the chemistry of clinopyroxenes in the ultramafic and mafic inclusions was investigated. The relationship between Al_2O_3 and FeO is shown in Text-fig. 26. Takasawa and Hirano (1977) have proposed a new method to infer the magma series using Al_2O_3 variation of clinopyroxene. They concluded that the Al_2O_3 content of Ca-pyroxene increases with increasing FeO_t in Ca-pyroxene in the alkaline rocks, whereas in the non-alkaline rocks it decreases or remains constant with increasing FeO_t in Ca-pyroxene. The Al_2O_3 variation with increasing FeOt for the clinopyroxene from Oshima-Ōshima is shown in Text-fig. 26. The observed chemical variation of the clinopyroxene in the inclusions has the following features: First Al_2O_3 increases from the dunite to clinopyroxenite inclusions which crystallized from the alkali basalt magma. Later Al_2O_3 decreases from the clinopyroxenite to hornblende grabbro inclusions, which crystallized from the magma changing from alkali basalt to calc-alkaline andesite.

Takasawa and Hirano (1977) explained Al_2O_3 variation of clinopyroxene crystallized from alkaline or non-alkaline magma using an equation shown below.

$$a^{Px}_{CaAl_2SiO_6} = K_{P,T)} \frac{a^{Pl}_{CaAl_2Si_2O_8}}{a^{liq}_{SiO_2}}$$

Since the plagioclase fractionation is delayed in the crystallization of basaltic magma in Oshima-Ōshima, the above equation is not suitable to use. It is better to use the activity of anorthite component in magma ($a_{CaAl_2Si_2O_8}$) instead of $a_{CaAl_2Si_2O_8}$. Therefore, the Al_2O_3 trend shown in clinopyroxenes (Text-fig. 26) is well interpreted as follows:

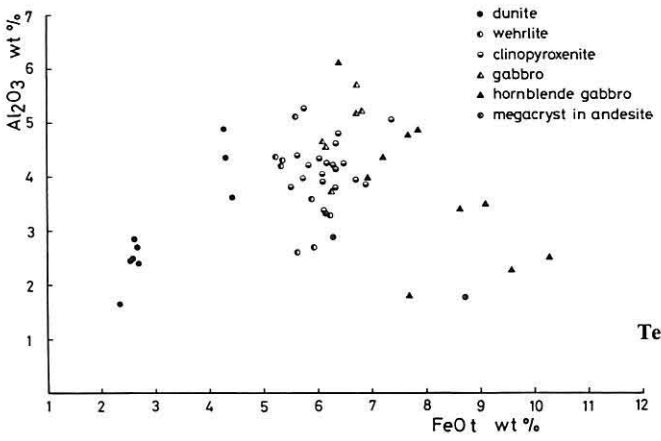

Text-fig. 26 FeO_t-Al_2O_3 diagram for the clinopyroxene in the ultramafic and mafic inclusions.

Since the basaltic magma increases abruptly in Al_2O_3 content with a slight SiO_2 enrichment, CaTs molecule in clinopyroxene increases from the dunite to clinopyroxenite. On the other hand, since the andesitic magma decreases slightly in Al_2O_3 content with a considerable SiO_2 enrichment, CaTs molecule considerably decreases from the clinopyroxenite to hornblende gabbro. Hence, the chemical variation of clinopyroxene also suggests the fractionation process discussed up to this point.

(6) Pressure conditions of crystallization of the basaltic magma

The chemistry of spinel and olivine is examined in order to deduce pessure conditions under which magmatic differentiation occurred in Oshima-Ōshima volcano.

Composition of spinel is controlled by various factors (bulk chemistry, pressure, temperature and oxygen fugacity) of the host magma (Irvine, 1965, 9167; Thompson, 1973; Hill and Roeder, 1974; Haggerty, 1979; Shiraki et al., 1979). It is therefore important to decide the main factor that controls the chemistry of spinel.

Nagao et al. (1980) who investigated the spinels in the Misasa alkali basalts and the Chōkai calc-alkali andesites, suggested that the chemistry of spinel is governed by the chemical composition of host magma as well as pressure. In a comment on this conclusion, Shiraki et al. (1981) stated that excess Al_2O_3 in spinel is affected by pressure rather than chemical composition of host magma. In a reply to this comment Nagao et al. (1981) pointed out the necessity in setting up a standard in judging "the excess Al_2O_3" and stated that normalizing the host rock chemistry by the SiO_2, Al_2O_3 and Cr_2O_3 contents is an effective method, when comparing spinel chemistries.

From this point of view, it is worthwhile investigating the composition of spinels that occur in basalts and in ultramafic inclusions cognate with basalts. Chemical data of the spinels are listed in Tables 7 and 8.

The relationship of the Al_2O_3 contents of bulk composition of basalts and those of spinels in the basalts are shown in Text-fig. 27. Since the separation of plagioclase from

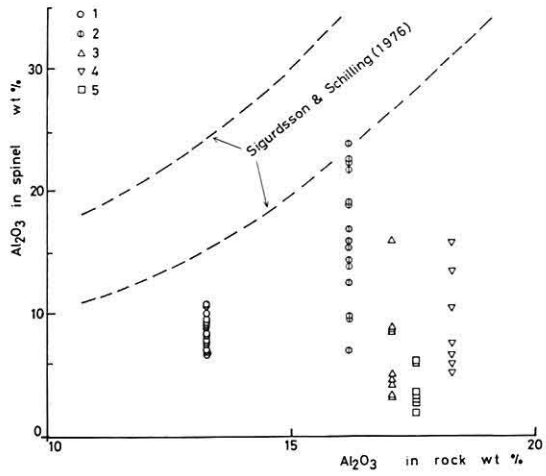

Text-fig. 27 Plot of Al_2O_3 content of spinels vs. Al_2O_3 content of whole rock.
1: augite-olivine basalt (Nu-104), 2: olivine-augite basalt (Ne-56), 3: olivine-augite basalt (Hu-100), 4: olivine-augite basalt (Cl-119), and 5: olivine-augite basaltic andesite (Nl-11e).

basaltic magma is delayed under the hydrous condition, the Al_2O_3 content increases as differtiation of basaltic magma proceeds (Yamamoto et al., 1977). The Al_2O_3 contents of the spinels in Nu-104 and Ne-56 seem dependent on the variation of the Al_2O_3 contents in the host basalts caused by differentiation. This is consistent with the observation of Sigurdsson and Schilling (1976) that the chemistry of spinels in MAR basalts depends on the chemistry of host rock. The Al_2O_3 contents are low in spinels rich in magnetite component; the spinels in Hu-100, Nl-14, and Cl-1119 are lower in Al_2O_3 content than in Nu-104 and Ne-56.

Text-fig. 28 shows a compositional variation of spinels from Cr- to Fe^{3+}-rich associated with an increase in the Al/Cr + Al ratio, and represents the crystallization course of spinel in the basalt. However, it is noteworthy that some low Fe^{3+} spinels in Ne-56 display an anomalous trend that reaches the area occupied by the spinels in the dunite.

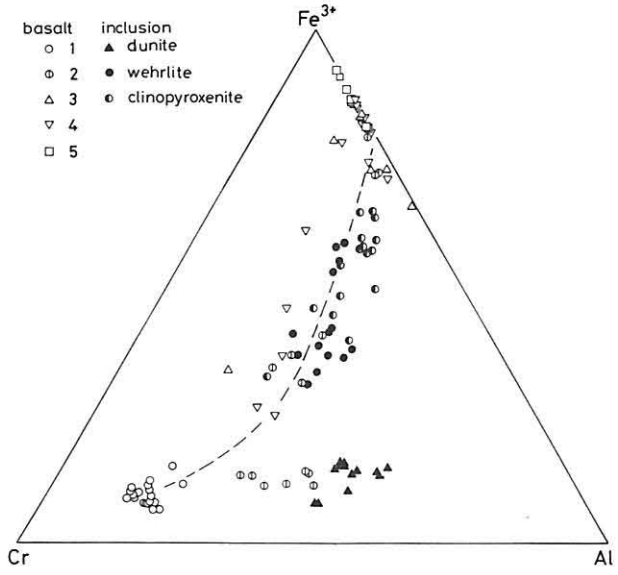

Text-fig. 28 Cr-Al-Fe^{3+} diagram of spinels.
1: augite-olivine basalt (Nu-104), 2: olivine-augite basalt (Ne-56), 3: olivine-augite basalt (Hu-100), 4: olivine-augite basalt (Cl-119), 5: olivine-augite basaltic andesite (Nl-14), and dunite, wehrlite, and olivine-clinopyroxenite.

Although spinels in the wehrlite and the olivine-clinopyroxenite have ratios of $Fe^{3+}/Cr + Al + Fe^{3+}$ more than 0.3 and are scattered over a wide range of Fe^{3+}, their trend is similar to that of the spinel in the basalts. On the other hand, spinels in the dunite plot apart from the trend of spinels in the wehrlite and olivine-clinopyroxenite.

The relationship between the ratio Mg/(Mg + Fe + Mn) and the CaO content of olivines in the basalts (Table 10) and the ultramafic inclusions (Table 4) is illustrated in Text-fig. 29. The CaO contents of olivines in the ultramafic inclusions are lower than those of the olivine phenocrysts in the basalts, and they only overlap slightly. According to Simkin and Smith (1970), the former can be classified into "inclusion and plutonic olivine" and the latter "extrusive and hypabyssal olivine". Simkin and Smith (1970) suggested a dependence of CaO content in olivine on pressure based on their

data on minor elements in olivine from various rock types. Stormer (1973) investigated the CaO zoning of olivine phenocrysts from volcanic rocks and stated that the pressure release during crystallization causes an increase of the CaO content in olivine and that stable pressure conditions do not lead to an increase in CaO content with an increase in FeO content. These authors pointed to a pressure dependence of CaO content in olivine. However, Takahashi (1979) argued that the CaO content is controlled by temperature.

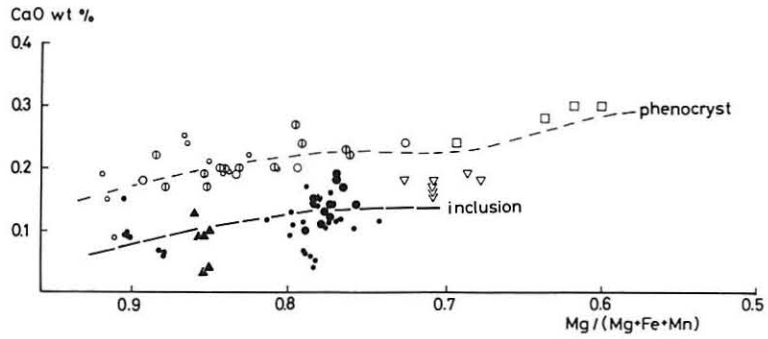

Text-fig. 29 CaO — Mg/(Mg + Fe + Mn) diagram for olivines. Symbols same as Text-fig. 28. large symbols indicate olivines in contact with spinels.

In Oshima-Ōshima, since the inclusions are cognate cumulates, if CaO content of olivine depends only on chemistry of magma, only one trend should be present in the CaO-Fo diagram of phenocryst and inclusion olivines. Two trends, however, are observed in Text-fig. 29, suggesting a pressure and/or temperature effect on the CaO content of olivines. The relationship of the $Mg/Mg+Fe^{2+}$ ratio of olivines and spinels in contact with each other is illustrated in Text-fig. 30. it shows a positive correlation. The spinels in Nu-104 have low $Mg/Mg+Fe^{2+}$ ratios, indicating that they are strongly affected by cooling. The relationship between the temperatue, calculated by olivine-spinel geothermometer (Roeder et al., 1979), and Fo content of the olivines, except Nu-104 and the spinels which have a ratio of $Fe^{3+}/Cr+Al+Fe^{3+}$ more than 0.4, are shown in Text-fig. 31. It is noticed that both phenocrysts and inclusions have the same trend as shown in Text-fig. 31. Therefore, the CaO content seems to be independent of temperature, and the difference in CaO content between phenocrysts and inclusions may be due to the difference of the pressure at which they crystallized.

Nevertheless, no distinct difference in the chemistry of spinels is observed, and the trends of spinels both in the basalts and inclusions (except dunite) overlap in the Cr-Al-Fe^{3+} diagram (Text-fig. 28). Therefore, it is more likely that spinel chemistry is controlled by the compositon of the host magma in the pressure range in which the phenocrysts and the wehrlite → olivine-clinopyroxenite inclusions are formed.

In Oshima-Ōshima volcano, the fractionated olivine-clinopyroxenite and hornblende gabbro inclusions, which played an important role in the differentiation of

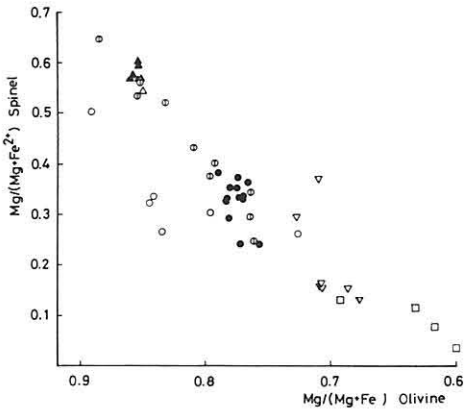

Text-fig. 30 Correlation between $Mg/Mg+Fe^{2+}$ values of spinels and olivines in contact with each other. Symbols same as Text-fig. 28.

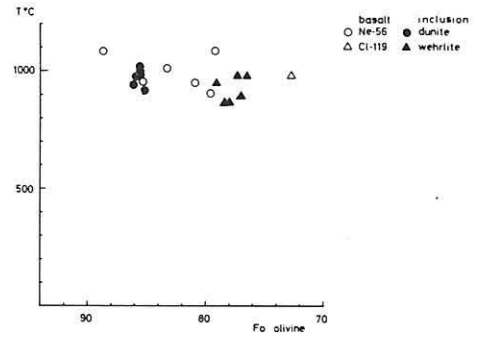

Text-fig. 31 Plot of calculated temperature by the method of Roeder et al. (1980) vs. Fo content of the olivine in contact with spinel.

basaltic magma to andesitic magma, would be formed at a shallow depth in the crust (Yamamoto et al., 1977). However, as stated before, spinels in the inclusions formed at such a low pressure have similar Al_2O_3 content to those included in olivine phenocrysts formed near the surface from the fractionated magma.

According to the experimental study on Apollo 14 rocks by Green et al. (1972), Al_2O_3 content of spinel increases about 7 wt% with an increase of pressure from 5 kb to 7 kb. Jaques and Green (1980) investigated the chemistry of spinels produced as a residual phase from the partial melting of peridotites, and stated that chrome spinels near the solidus at low pressure (2-5 kb) were distinctly more chrome-rich than those at higher pressure (10-15 kb). Their experimental data showed that the difference in $Cr/Cr+Al$ ratio of the spinels over a pressure range of 3 kb (2 kb-5 kb) is slight.

In Oshima-Ōshima, the dunite inclusions are found in small amounts and they are small in size (2×3 cm). Their olivines have an angular shape, while the olivines in other inclusions do not. The olivines included in the dunite always show kink-banding. Therefore, the dunite inclusions may be formed as fractionation products from magma at deeper levels than the other inclusions, as mentioned earlier. Furthermore Al_2O_3 contents of spinels in the dunite are 12 to 20 wt% higher than those in the wehrlite and the olivine-clinopyroxenite in clusions. Judging from the experimental result of Jaques and Green (1980), this difference in Al_2O_3 content of spinel is due to the pressure rather than the bulk composition of host liquid. Some olivine phenocrysts in the basalts may be derived from the dunite inclusion: for example those in sample Ne-56 which has more aluminous trend of spinels (Text-fig. 28) and KD less than 0.3 (Roeder and Emslie, 1970).

Table 10 Selected microprobe analyses of the olivines in the basalts

Sp.no.	1 Nu-105- 14	2 Nu-105- 18	3 Nu-K37- 6	4 Nu-K37- 7	5 Nu-104- 1	6 Nu-104- 4	7 Ne-56- 9	8 Ne-56- 2	9 Cl-119- 1	10 Cl-119- 2	11 Nl-14- 2	12 Nl-14- 3
SiO_2	40.73	41.01	40.82	41.18	39.85	40.77	39.91	39.92	38.93	38.32	37.29	35.78
TiO_2	—	—	—	—	0.02	0.07	—	—	—	—	—	—
Al_2O_3	—	—	—	—	0.10	0.04	—	—	—	—	—	—
FeO	6.69	7.28	6.20	6.99	7.49	7.89	13.88	18.79	24.44	25.79	27.48	34.49
MnO	—	—	—	—	0.15	0.15	0.17	0.31	0.50	0.65	0.57	0.93
MgO	50.59	50.63	50.93	50.96	50.25	50.86	45.41	41.52	37.57	36.09	34.75	29.03
NiO	0.45	0.42	0.47	0.44	0.40	0.33	0.16	0.00	0.09	0.08	0.00	0.00
CaO	0.07	0.12	0.14	0.16	0.19	0.15	0.17	0.27	0.18	0.17	0.29	0.30
Total	98.53	99.46	98.56	99.74	98.46	100.27	99.70	100.81	101.51	101.08	100.38	100.53
Numbers of cations on the basis of 4 oxygens												
Si	1.000	1.000	1.000	1.000	0.986	0.990	1.000	1.011	1.007	1.003	0.993	0.998
Al	—	—	—	—	0.003	0.001	—	—	—	—	—	—
Ti	—	—	—	—	0.000	0.001	—	—	—	—	—	—
Fe	0.137	0.148	0.127	0.142	0.155	0.160	0.291	0.398	0.528	0.565	0.612	0.797
Mn	—	—	—	—	0.003	0.003	0.004	0.007	0.011	0.014	0.013	0.022
Mg	1.852	1.840	1.860	1.845	1.853	1.842	1.697	1.567	1.440	1.408	1.380	1.196
Ni	0.009	0.008	0.009	0.009	0.008	0.006	0.003	0.000	0.002	0.002	0.000	0.000
Ca	0.002	0.003	0.004	0.004	0.005	0.004	0.005	0.007	0.005	0.005	0.008	0.009
Total	3.000	2.999	3.000	3.000	3.013	3.007	3.000	2.990	2.993	2.983	3.006	3.012
$\frac{100 \times Mg}{Mg+Fe}$	93.4	92.9	93.6	92.9	92.1	91.9	85.4	79.7	72.8	70.9	69.3	60.0

1-4: analyzed by simple method using the calculated α factors for endmembers of olivine molecule.
Calculation method by Yusa and Tsuzuki (1976).

Origin of the calc-alkaline andesite of Oshima-Ōshima volcano

Origin of the calc-alkaline andesite of Oshima-Ōshima volcano

Volcanic rocks from Oshima-Ōshima volcano consist mainly of alkali olivine basalt and hornblende-hypersthene-augite andesite of the calc-alkaline rock series, the latter of which is characterized by the presence of groundmass orthopyroxene and by no iron enrichment (Text-fig. 8). Furthermore, the weight ratio of $FeO + Fe_2O_3/FeO + Fe_2O_3 + MgO$ in this calc-alkaline andesite increases only slightly compared with that in the alkalic basalt series (Text-fig. 32). The alkali basalt and calc-alkaline andesites from Oshima-Ōshima are intimately associated with each other, even within a single cycle of eruption as in the recorded eruption in 1741-1742. Almost continuous variation curves of major elements can be traced from the basalt to andesite without notable break.

Differences in chemical compositions between the alkali basalt and the calc-alkaline andesite are summarized as follows: (1) In the basaltic rocks, SiO_2, content increases only slightly with proceeding differentiation of the basaltic magma. In the andesitic rocks, however, SiO_2 content abruptly increases with differentiation of the magma. (2) Alkali, Rb and Ba contents increase in the basalt whereas they remain constant from the felsic basalt to the mafic andesite. (3) The rate of increase of Al_2O_3 content in the basaltic rocks is high, whereas the rate in the andesitic rocks becomes near zero then decreases.

These chemical variations suggest the following petrogenesis: The amphibole may appear as a near liquidus phase in the hydrous felsic basalt magma ($SiO_2 = 51\%$) which is the most differentiated magma in the basaltic range. Consequently, amphibole fractionation (hornblendite inclusion) followed by amphibole + plagioclase fractionation (hornblende gabbro inclusion) results in the generation of the calc-alkaline andesitic magma. Since the amphiboles from Oshima-Ōshima are poor in SiO_2 and rich in alkali, the hornblendite and hornblende gabbro inclusions are highly nepheline- and leucite-normative. Therefore, the hornblendite and hornblende gabbro fractionation from the alkali basalt magma effectively leads to the calc-alkaline andesite.

The variation in iron ratio of the Oshima-Ōshima rocks is also consistent with the above considerations. Text-fig. 32 shows that:

(1) The primary magma, which is picritic and hydrous, crystallizes mainly olivine to form dunite inclusions, then the fractionation products become rich in clinopyroxene as inferred from the wehrlite and clionopyroxenite inclusions. This fractionation process can be well interpreted by the subtraction diagram (Text-fig. 19) and the calculation of FeO-MgO distribution between olivine and rock (Roedder and Emslie, 1970) (solid tie-lines in Text-fig. 32).

(2) Consequently the magma is chemically changed into the felsic basalt magma ($= SiO_2$ 51%). The amphibole may appear as a near liquidus phase in the hydrous felsic basalt magma. Since amphibole is in reaction relation with olivine and clinopyroxene, it crystallizes alone at first. Then, crystallization of plagioclase ensues.

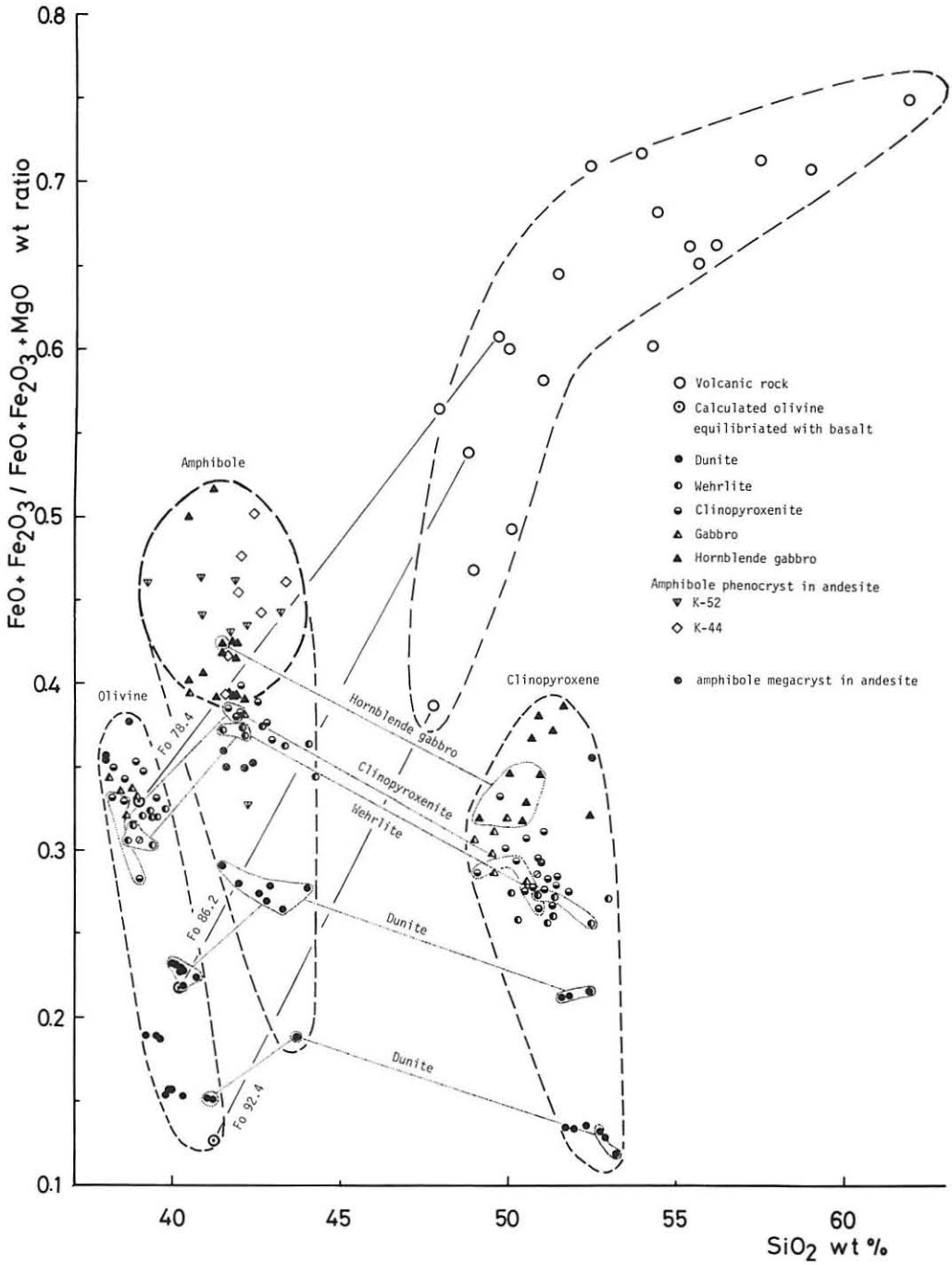

Text-fig. 32 $FeO + Fe_2O_3/MgO + FeO + Fe_2O_3$) vs. Sio_2 diagram for basalt-andesite suite and minerals in the ultramafic & mafic inclusions from Oshima-Ōshima. Dotted tie lines show the same specimens of the inclusions.

During the crystallization, the magma does not increase in the ratio of $FeO+Fe_2O_3/FeO+Fe_2O_3+MgO$, because amphibole is high in this ratio. Consequently, the variation in the volcanic rocks from alkaline basalt to calc-alkaline andesite is considered to have been caused by amphibole fractionation under hydrous condition at a shallow level in the continental crust. This fractionation is considered to be essential to the genesis of the calc-alkaline andesite from Oshima-Ōshima, whereas effect of magnetite fractionation may be very small.

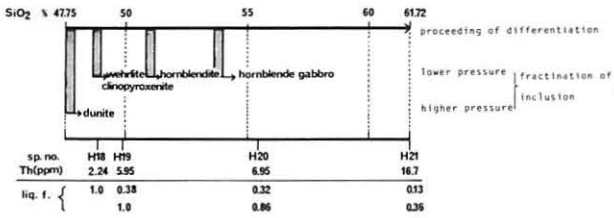

Text-fig. 33 Crystallization sequence of the basaltic-andesitic magma in Oshima-Ōshima. The Th content were determined by Masuda et al. (1975).

The crystallization sequence of the magma in Oshima-Ōshima volcano is illustrated in Text-fig. 33. The liquid fraction can be calculated using Th content as a measure of liquid fraction "f" by the method of Allègre et al. (1977). This element has been called hygromagmatophile (Treuile and Varet, 1973) or H element (Allègre et al., 1977). The differentiation of magma can be approximated by using Th, which generally has a great affinity for the liquid. The Th content determined for 4 rocks by Masuda et al. (1975) and the liquid fraction assuming H_{18}basalt as a initial liquid are shown in Text-fig. 33. The liquid fraction of H_{20} is calculated at 0.32. Although it is considered that the primary magma in Oshima-Ōshima is not represented by H_{18} but the picritic basalt (Nishi-yama upper lava: $SiO_2=47.75\%$) in chemical composition, the value of the liquid fraction of H_{20} (a typical calc-alkaline andesite) is consistent with the field evidence of the volcano that about 30 vol.% of the volcanic rocks are calc-alkaline andesite and the rest are alkali olivine basalt.

The stages at which the fractionation of some inclusions took place are shown in Text-fig. 33. It is concluded that:

(1) The ultramafic and mafic inclusions from Oshima-Ōshima volcano are products crystallized from basaltic magma and are cognate inclusions with the volcanic rocks.

(2) The inclusions have formed at a shallower level in the continental crust, except the dunite inclusion which has formed at a deeper level as inferred from its occurrence and mineralogy.

(3) They have played an important role in fractional crystallization of the basaltic magma of Oshima-Ōshima volcano.

(4) The amphibole fractionation (hornblendite and hornblende gabbro fractionation) occurred from the felsic basalt magma, which is noticed as an important factor for the genesis of calc-alkaline andesite series.

The calc-alkaline andesite of the Chōkai Volcanic Zone

In the AFM diagram (Text-fig. 8), the chemical composition of the calc-alkaline rocks from Oshima-Ōshima volcano plot within the fields of those from other volcanoes of the Chōkai Volcanic Zone. These common chemical features may suggest that the calc-alkaline andesite from Oshima-Ōshima volcano has a genetic relation to those from the other volcanoes of the Chōkai Volcanic Zone.

On the basis of above assumption, the general features of the chemistry and the petrography for the rocks of the Chōkai Volcanic Zone including Oshima-Ōshima volcano were examined and compared with those of the Nasu Volcanic Zone. The Quaternary volcanic rocks in Northern Japan are grouped in a basalt-andesite-dacite-rhyolite suite, of which andesite and dacite of the calc-alkaline series are generally abundant rocks as in other island arc areas. These rocks vary markedly in nature from the Pacific side (calcic to low-potassic) to the Japan Sea side (more alkalic and high-potassic) of the arc. The volcanoes of the Nasu Volcanic Zone are distributed on the Pacific side, whereas those of the Chōkai Volcanic Zone are on Japan Sea side. Accordingly, the rocks of the Chōkai Volcanic Zone are higher in alkali content than those of the Nasu Volcanic Zone.

SiO_2 frequency-distribution for the rocks from the Chōkai Volcanic Zone (Oshima-Ōshima volcano and the others) and the Nasu Volcanic Zone is shown in Text-fig. 34. Chemical and petrographical data are from Kawano et al. (1961), Ōnuma (1963) and Togashi (1977). It is noticed that:

(1) In the Nasu Volcanic Zone, both tholeiitic rocks and calc-alkaline rocks have a wide range of SiO_2 contents. Furthermore, the of SiO_2 contents in calc-alkaline rocks is different from that in tholeiitic rocks. In the Chōkai Volcanic Zone, however, the rocks of high-alumina basalt series or alkali basalt series (Oshima-Ōshima) are low in SiO_2 content, whereas those of calc-alkaline series are high in SiO_2, content. In other

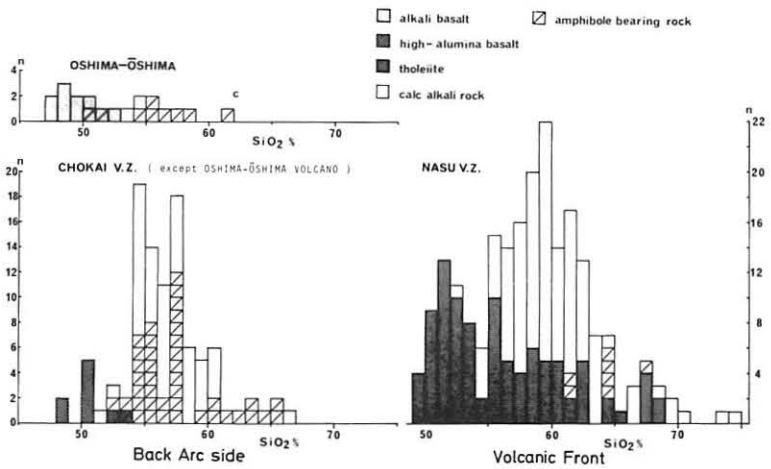

Text-fig. 34 Silica-frequency diagram for the rocks from the Chōkai Volcanic Zone and Nasu Volcanic Zone.

words, there is little overlap in SiO_2 contents of the two rock types.

(2) Amphiboles are associated with the dacite in the Nasu Volcanic Zone, whereas they are associated with the andesite, and even with the basalt, in the Chōkai Volcanic Zone.

The above observations suggest that the crystallization course of the calc-alkaline magma is different from that of the tholeiite magma in the Nasu Volcanic Zone. In the Chōkai Volcanic Zone the calc-alkaline magma may be produced by amphibole fractionation from a hydrous basalt magma. As well known, the rocks of Chōkai Volcanic Zone frequently include many amphibole phenocrysts.

The amphiboles from Chōkai volcano were analyzed by microprobe to compare with those from Oshima-Ōshima volcano. The analytical data are listed in Table 11. According to the data, the amphiboles from Chōkai volcano are poor in Si, as are from Oshima-Ōshima, and are classified into pargasite or pargasitic hornblende. On the other hand, the amphiboles from the dacite of Osore-yama volcano (Nasu Zone) are rich in Si and classified as common hornblende (Togashi, 1977).

Sakuyama (1977) examined the lateral variation of mafic phenocryst assemblages in rocks in northeastern Japan and pointed out that the magmas under the area are not satuated with H_2O, although the H_2O contents in the rocks increase away from the volcanic front. It is an important fact that the pargasites are associated with the basalts, as mentioned above. The basaltic magmas in the Chōkai Volcanic Zone are more hydrous than those in the Nasu Volcanic Zone and crystallize the Si-poor amphibole.

The wet and alkalic nature of the magmas are important factors for the stability of amphibole (Cawthorn, 1976; Cawthorn and O'Hara, 1976). These are indispensable conditions under which the basaltic magma fractionates amphiboles at an early stage of differentiation. The petrochemistry and petrography of the rocks from the Chōkai Volcanic Zone seem to meet the above conditions.

High-alumina basalts from Chōkai volcano are felsic and are similar to the felsic basalt from Oshima-Ōshima. Such a magma is considered capable of crystallizing amphiboles as a liquidus phase. Accordingly, it is probable that the mafic andesite, which is abundant in Chōkai volcano, is produced from the high-alumina basalt magma by such an amphibole fractionation process. The high-alumina basalt magma would effectively increase in SiO_2 content by the fractionation of amphibole, because the amphibole is highly nepheline-normative.

If H_{19}, which is analogous to the high-alumina basalt magma of Chōkai volcano, can be used as an initial liquid, then the residual liquid fraction of H_{20} (mafic andesite) is calculated as 0.86 (Text-fig. 33). this value supports the abundance of mafic andesite in Chōkai volcano.

Accordingly, it is possible that the calc-alkaline andesites from the Chōkai Volcanic Zone are produced by amphibole fractionation from the basaltic magma at an early stage of differentiation.

Fluorine generally has a great affinity for amphibole and apatite. Aoki (1978) investigated the F concentration in the volcanic rocks from Nasu Volcanic Zone, Chōkai

Table 11 Microprobe analyses of amphiboles from Chōkai Volcano

	1	2	3	4	5	6	7
sp.no.	1C-102	1C-1-3	1C-1-4	1C-3-1	1C-3-2	1C-3-3	1C03-5
SiO_2	41.70	41.45	41.50	42.88	42.49	41.77	42.27
TiO_2	2.82	2.80	2.81	2.88	3.40	3.05	2.62
Al_2O_3	13.69	13.98	12.15	11.45	11.47	11.45	11.31
FeO	9.59	9.49	11.14	11.52	11.75	11.72	12.08
MnO	0.11	0.18	0.13	0.09	0.07	0.08	0.10
MgO	14.70	14.30	14.29	14.20	14.13	13.73	14.75
CaO	11.77	11.36	11.46	11.27	11.30	11.29	11.03
Na_2O	2.32	2.22	2.30	2.19	2.17	2.05	2.10
K_2O	0.77	0.70	0.73	0.57	0.62	0.60	0.56
Total	97.47	96.48	96.51	97.05	97.40	95.74	96.82
Numbers of cations on the basis of 23 oxygens							
Si	6.100	6.111	6.182	6.331	6.268	6.272	6.278
Al^{IV}	1.900	1.889	1.818	1.669	1.732	1.728	1.722
Al^{VI}	0.461	0.540	0.315	0.324	0.262	0.298	0.258
Ti	0.310	0.310	0.315	0.320	0.377	0.344	0.293
Fe	1.173	1.170	1.388	1.422	1.449	1.472	1.500
Mn	0.014	0.023	0.016	0.011	0.009	0.010	0.013
Mg	3.206	3.143	3.173	3.126	3.107	3.074	3.266
Ca	1.845	1.795	1.829	1.783	1.786	1.816	1.755
Na	0.658	0.635	0.664	0.627	0.621	0.597	0.605
K	0.144	0.132	0.139	0.107	0.117	0.115	0.106
Total	15.811	15.748	15.839	15.720	15.728	15.726	15.526
Ca	29.6	29.3	28.6	28.1	28.1	28.5	26.9
Mg	19.0	19.5	21.9	49.3	48.9	48.9	50.0
Fe + Mn	51.4	51.2	49.5	22.6	23.0	23.3	23.1
$\frac{100 \times Mg}{MG + Fe + Mn}$	73.0	72.5	69.3	68.6	67.5	67.5	68.3

1-3: hornblende-bearing olivine-hypersthene-augite andesite
4-7: hornblende-bearing hypersthene-olivine-augite andesite
Rock smaples from K. Ōnuma.

Volcanic Zone and Iki island. F content in the rocks from Nasu Volcanic Zone increases with increasing SiO_2 content, whereas that from Chōkai Volcanic Zone and Iki island increases only slightly. It was interpreted by Aoki (1978) that the latter trend is caused by hornblende- and biotite-fractionation. This supports the above discussions of the amphibole fractionation for the genesis of calc-alkaline andesite.

Conclusion

(1) Oshima-Ōshima volcanic island is situated off the Japan Sea coast, southwest Hokkaido, and consists of a triple stratovolcano.

(2) The volcanic edifice is made up of lavas and pyroclastics, of which about 30 vol.% is calc-alkaline andesite and the rest is alkali olivine basalt. The andesite and basalt are intimately associated with each other, even within a single cycle of eruption as in the recorded eruption in 1741-1742.

(3) In major element and trace element chemistry of the rocks from Oshima-Ōshima, almost continuous variation curves can be traced from basalt to andesite without notable break. Both the alkali olivine basalt and calc-alkaline andesite have higher alkali contents.

(4) Most of the andesites and some basalts contain ultramafic and mafic inclusions such as dunite, wehrlite, olivine clinopyroxenite, hornblendite, and hornblende gabbro, which show a typical cumulate texture. Occurrence, textue and chemistry of minerals of the inclusions suggest that they are products crystallized from a basaltic magma and are cognate with the basalt-andesite suite of Oshima-Ōshima volcano. These inclusions have played an important role in the fractional crystallization of the basaltic magma of Oshima-Ōshima volcano.

(5) The different trends of oxide variation between the basalts and andesites have resulted from the different crystallization sequence between both rock suites. The crystallization sequence of the ultramafic and mafic inclusions is as follows: dunite → wehrlite → olivine-clinopyroxenite → clinopyroxenite → hornblendite → hornblende gabbro. The chemical variation trend from the picritic basalt to the felsic basalt is interpreted by the successive removal of the dunite, wehrlite and clinopyroxenite compositions, whereas the trend from the felsic basalt to the andesite is explained by the successive removal of hornblendite and hornblende gabbro compositions.

(6) The phase relationships of basalt-andesite in some synthetic or natural systems and the comparison of mineral chemistry between the volcanic rocks and the inclusions suggest that dunite fractionation from the primary magma took place at a higher pressure under hydrous conditions, whereas the other fractionation took place at shallow levels in the continental crust under hydrous conditions.

(7) The variation in the volcanic rocks from alkaline basalt to calc-alkaline andesite was caused by amphibole fractionation under hydrous conditions at shallow levels in the continental crust.

(8) The estimated rate of the residual liquid fractions is consistent with the field observation that about 30 vol.% of the volcanic rocks are andesites and the rest are basalts.

(9) The wet and alkalic nature of the magmas are important factors for the stability of amphiboles. These are indispensable conditions under which basaltic magma crystallizes amphibole at an early stage of differentiation. The petrochemistry and petrography of the rocks from the Chōkai Volcanic Zone seem to meet these conditions. Therefore, it is possible that the calc-alkaline andesites from the Chōkai

Volcanic Zone are produced by amphibole fractionation from the basaltic magma.

Acknowledgements

I wish to express my sincere thanks to Prof. Y. Katsui of Hokkaido University for his continuous guidance and encouragement. I also wish to express my appreciation to Dr. K. Niida of the same university and to Dr. K. Onuma of Tohoku University and Dr. T. Nagao of Yamaguchi University for their valuable suggestions. I am grateful to Dr. J. Nishikawa of Civil Engineering Research Institute, Sapporo, and Mr. S. Nemoto of Seya-nishi High School, Yokohama for trace element analysis and to Mr. K.T.M. Johnson of Hokkaido University for a critical reading of the manuscript.

Acknowledgements must be made to Drs. Y. Suzuki and S. Yokoyama of Government Industrial Development, Hokkaido, and to Drs. K. Okumura, T. Soya, and H. Satoh of the Geological Survey of Japan for their kind assistance with EPMA analysis. Thanks are also due to Messrs. K. Moribayashi and T. Kuwajima, and Mrs. S. Yokoyama of Hokkaido University for their providing thin sections and her typing the manuscript.

References

Albarède, F., 1976. Some trace element relationships among liquid and solid phases in the course of the fractional crystallization of magma. *Geochim. Cosmochim. Acta*, 40: 667-673.

Allègre, G.J., Treuile, M., Minster, J.F., Minster, B. and Albarède, F., 1977. Systematic use of trace element in igneous process part I: Fractional crystallization processes in volcanic suites. *Contr. Min. Petr.*, 60: 57-75.

Allen, J.C., Boettcher, A.L. and Marland, G., 1975. Amphiboles in andesite and basalt: I. Stability as a function of P-T-fO_2. *Am. Min.*, 60: 1069-1085.

Aoki, K., 1978. The origin of volcanic rock in Japanese Island. In: *Earth Science 3*, I. Kushiro and S. Aramaki (eds.), Iwanami, Tokyo, pp. 153-182 (in Japanese).

Banno, S. and Yamazaki, M., 1979. Behavior of large divalent cations during fractional crystallization in a model system diopside-albite-anorthite. *Chem. Geol.*, 24: 243-257.

Bence, A.E. and Albee, A.L., 1968. Empirical correction factors for the electron microanalysis of silicates and oxides. *Jour. Geol.*, 76: 382-403.

Cawthorn, R.G., Curran, E.B. and Arculus, R.J., 1973. A petrogenitic model of the origin of the calc-alkaline suite of Grenada, Lesser Antilles. *Jour. Petr.*, 14: 327-337.

Cawthorn, R.G. and O'Hara, M.J., 1976. Amphibole fractionation in calc-alkaline magma genesis. *Am. Jour. Sci.*, 276: 309-329.

Cawthorn, R.G. 1976. Melting relations in part of the system CaO-MgO-Al_2O_3-SiO_2-Na_2O-H_2O under 5 kb pressure. *Jour. Petr.*, 17: 44-72.

Clarke, D.B., 1970. Tertiary basalts of Baffin Bay: possible primary magma from the mantle. *Contr. Min. Petr.*, 25: 203-224.

Cox, K.G. and Bell, J.D., 1972. A crystal fractionation model for the basaltic rocks of the New Georgia Group, British Solomon Islands. *Contr. Min. Petr.*, 37: 1-13.

Cox, K.G. and Hornung, G., 1966. The petrology of the Karroo basalts of Basutoland. *Am. Min.*, 51: 1414-1432.

Deer, W.A., Howie, R.A., and Zussman, J., 1966. *An Introduction to the Rock Forming Minerls*. Longman Group Limited, London, pp. 528.

Green, D.H. and Ringwood, A.E., 1968. Genesis of the calc-alkaline igneous rock suite. *Contr. Min. Petr.*, 18: 105-162.

Green, D.H. Ringwood, A.E., Ware, N.G. and Hibberson, W.O., 1972. Experimental petrology and petrogenesis of Apollo 14 basalts. *Proc. Third Lunar Sci. Conf., Geochim. Cosmochim. Acta*, Suppl. 3, (1): 197-206.

Haggerty, S.E., 1979. Spinels in high pressure regimes. In: F.R. Boyd and H.O.A. Meyer (eds.). *Inclusions in Kimberlites and Other Volcanics vol. 2*. Am. Geophys. Union: pp. 183-196.

Hatori, T. and Katayama, M., 1977. Tsunami behavior and source areas of historical tsunamis in the Japan Sea. *Bull. Earthq. Res. Inst.*, 52: 49-70 (in Japanese with English abstract).

Helz, R.T., 1973. Phase relations of basalts in their melting range at P_{H_2O} = 5 kb as a function of oxygen fugacity. Part I. mafic phases. *Jour. Petr.*, 14: 249-302.

Higuchi, H. and Nagasawa, H., 1969. Partition of trace elements between rock-forming minerals and the host volcanic rocks. *Earth Planet. Sci. Lett.*, 7: 281-287.

Hill, R. and Roeder, P., 1974. The crystallization of spinel from basaltic liquid as a function of oxygen fugacity. *Jour. Geol.*, 82: 709-729.

Holloway, J.R. and Burnham, C.W., 1972. Melting relations of basalt with equilibrium water pressure less than total pressure. *Jour. Petr.*, 13: 1-29.

Irvine, T.N., 1965. Chromian spinel as a petrogenetic indicator, Part 1. Theory. *Can. Jour. Earth Sci.*, 2: 648-672.

Irvine, T.N., 1967. Chromian spinel as a petrogenetic indicator, Part 2. Petrologic applications. *Can. Jour. Earth Sci.*, 4: 71-103.

Jaques, A.L. and Green, D.H., 1980. Anhydrous melting of peridotite at 0-15 kb pressure and genesis of tholeiitic basalts. *Contr. Min. Petr.*, 73: 287-310.

Jensen, B.B., 1973. Patterns of trace element partitioning. *Geochim. Cosmochim. Acta*, 37: 2227-2242.

Kanisawa, S., 1972. Coexisting biotites and hornblendes from some granitic rocks in southern Kitakami Mountains, Japan. *Jour. Japan Assoc. Min. Petr. Econ. Geol.*, 67: 332-344.

Kanisawa, S., 1975. Chemical composition of hornblendes of some Ryoke granites, central Japan. *Jour. Japan Assoc. Min. Petr. Econ. Geol.*, 70: 200-211.

Kanisawa, S., 1976. Chemistry of biotites and hornblendes of some granitic rocks in the San'in Zone, southwest Japan, *Jour. Geol. Soc. Japan*, 78: 39-49 (in Japanese with english abstract).

Katsui, Y. and Satoh, H., 1970. *Geology of the Oshima-Ōshima district*. Geol. Surv. Japan, Kawasaki, 216+4 pp (in Japanese with English abstract).

Katsui, Y., Yokoyama, I., Ehara, S., Yamashita, H., Niida, K., and Yamamoto, M., 1977. *Oshima-Ōshima. Report of the Volcanoes in Hokkaido, Part 6*. Committee for Prevention of Natural Disasters of Hokkaido, Sapporo, 82 pp (in Japanese).

Katsui, Y., Oba, Y., Ando, S., Nishimura, S., Masuda, Y., Kurasawa, H., and Fujimaki, H., 1978. Petrochemistry of the Quaternary volcanic rocks of Hokkaido, north Japan. *Jour. Fac. Sci., Hokkaido Univ., Ser. IV*, 18: 449-484.

Katsui, Y., Yamamoto, M., Nemoto, S. and Niida, K., 1979. Genesis of calc-alkalic andesites from Oshima-Ōshima and Ichinomegata volcanoes, north Japan. *Jour. Fac. Sci., Hokkaido Univ., Ser. IV*, 19: 157-168.

Katsui, Y. and Yamamoto, M., 1981. The 1741-1742 activity of Oshima-Ōshima volcano, north Japan. *Jour. Fac. Sci., Hokkaido Univ., Ser. IV*, 19: 527-536.

Kawano, Y., Yagi, K. and Aoki, K., 1961. Petrography and petrochemistry of the volcanic rocks of Quaternary volcanoes of northeastern Japan. *Sci. Rep. Tohoku Univ., Ser III*, 7: 1-40.

Kuno, H., 1936. Lavas from Oshima-Ōshima Volcano, Hokkaido. *Jour. Geol. Soc. Japan*, 43: 392-393 (in Japanese).

Kuno, H., 1950. Petrology of the Hakone Volcano and adjacent areas, Japan. *Bull. Geol. Soc. Am.*, 61: 957-1020.

Kuno, H., 1954. *Volcanoes and volcanic rocks*. Iwanami, Tokyo, pp. 255 (in Japanese).

Kuno, H., 1966. Lateral variation of basalt magma type across continental margins and island arcs. *Bull. Volc.*, 29: 195-222.

Leake, B.E., 1968. A catalogue of analyzed calciferous and subcalciferous amphiboles together with their nomenclature and associated minerals. *Geol. Soc. Am. Spec. Pap.*, 98: 210 pp.

Lewis, J.f., 1973a. Petrology of ejected plutonic blocks of the Soufriere volcano, St. Vincent, West Indies. *Jour. Petr.*, 14: 81-112.

Lewis, J.F., 1973b. Mineralogy of the ejected plutonic blocks of the Soufriere volcano, St. Vincent: olivine, pyroxene, amphibole and magnetite paragenesis. *Contr. Min. Petr.*, 38: 197-220.

Masuda, Y., Nishimura, S., Ideda, T. and Katsui, Y., 1975. Rare-earth and trace elements in the Quaternary volcanic rocks of Hokkaido, Japan. *Chem. Geol.*, 15: 251-271.

Matsui, Y., Onuma, N., Nagasawa, H., Higuchi, H. and Banno, S., 1977. Crystal structure control in trace element partition between crystal and magma. *Bull. Soc. Fr. Min. Cryst.*, 100: 315-324.

Nagao, T., Yamamoto, M. and Onuma, K., 1980. Crystallization trend of chromian spinel in some alkali basalts and calc-alkali andesites from Japanese Island. *Jour. Japan Assoc. Min. Petr. Econ. Geol.*, 75: 44-54.

Nagao, T., Yamamoto, M. and Onuma, K., 1981. A reply to the discussion on "Crystallization trend of chromian spinel in some alkali basalts and calc-alkali andesites from Japanese Island". *Jour. Japan Assoc. Min. Petr. Econ. Geol.*, 76: 30-33.

Nagasasa, H. and Schnetzler, C.C., 1971. Partition of rare earth, alkali and alkaline earth elements between phenocrysts and acidic igneous magma. *Geochim. Cosmochim. Acta*, 35: 953-968.

Nicholls, I.A., 1971. Petrology of Santorini volcano, Cyclades, Greece. *Jour. Petr.*, 12: 67-119.

Obata, M., Banno, S. and Mori, T., 1974. The iron-magnesium partitioning between naturally occuring coexisting olivine and Ca-rich clinopyroxene: an application of the simple mixture model to olivine solid solution. *Bull. Soc. Fr. Min. Crist.*, 97: 101-107.

O'Hara, M.J., 1965. Primary magmas and the origin of basalts. *Scot. Jour. Geol.*, 1: 19-44.

O'Hara, M.J., 1968. The bearing of phase equilibria studies in synthetic and natural systems on the origin and evolution of basic and ultrabasic rocks. *Earth Sci. Rev.*, 4: 69-133.

Ōnuma, K., 1963. Geology and petrology of Chokai volcano, northeastern Japan. Part II, petrochemistry and petrogenes (1). *Jour. Japan Assoc. Min. Petr. Econ. Geol.*, 50: 235-244.

Roeder, P.L. and Emslie, R.F., 1970. Olivine-liquid equilibrium. *Contr. Min. Petr.* 29: 275-289.

Roeder, P.L., Campell, I.H. and Jamieson, H.E., 1979. A re-evaluation of the olivine-spinel geothermometer. *Contr. Min. Petr.*, 68: 325-334.

Sakuyama, M., 1977. Lateral variation of H_2O contents in Quaternary magma of northeastern Japan. *Bull. Volc. Soc. Japan*, 2nd ser., 22: 263-271 (in Japanese with English abstract).

Sato, T. and Yoneyama Research Group, 1975. Volcanic rocks in the Yoneyama district, Niigata Prefecture, Japan. *Chikyu Kagaku, Jour. Assoc. Geol. Collab. Japan*, 29: 211-226 (in Japanese with English abstract).

Shiraki, K., Yusa, Y., Kuroda, N. and Ishioka, K., 1977. Chrome-spinels in some basalts from Guam, Mariana island arc. *Jour. Geol. Soc. Japan*, 83: 33-40 (in Jpanese with English abstract).

Shiraki, K., Ohashi, F. and Kuroda, N., 1979. Chrome-spinels in a basanitic lava from Nanzaki Volcano, Izu Peninsula. *Jour. Japan Assoc. Min. Petr. Econ. Geol.*, 74: 114-121 (in Japanese with English abstract).

Shiraki, K., Ohashi, F. and Kuroda, N., 1981. Comment on "Crystallization trend of chromian spinel in some alkali basalts and calc-alkali andesites from Japanese Island". *Jour. Japan. Assoc. Min. Petr. Econ. Geol.*, 76: 26-29.

Sigurdsson, H. and Shepherd, J.B., 1974. Amphibole-bearing basalts from the submarine volcano Kich'em-Jenny in the Lesser Antilles Island Arc. *Bull. Volc.*, 38: 891-910.

Sigurdsson, H. and Schilling, J.G., 1976. Spinels in Mid-Atlantic Ridge basalts; chemistry and occurrence. *Earth Planet. Sci. Lett.*, 29: 7-20.

Simkin, T. and Smith, J.V., 1970. Minor-element distribution in olivine, *Jour. Geol.*, 78: 304-325.

Stormer, J.C., Jr., 1973. Calcium zoning in olivine and its relationship to silica activity and pressure. *Geochim. Cosmochim. Acta*, 73: 1815-1821.

Sweatman, T.R. and Long, J.V.P., 1969. Quantitative electronprobe microanalysis of rock forming minerals. *Jour. Petr.*, 10: 332-379.

Takahashi, E., 1979. Thermal history of lherzolite xenolith (Petrology of lherzolite xenolith from Ichinomegata Crater: Part II) (Abstract). *Bull. Volc. Soc. Japan*, 2nd Ser., 24: 107-108 (in Japanese).

Takasawa, K. and Hirano, H., 1977. Some considerations on the relations between magma series and Al_2O_3 variation of Ca-pyroxene. *Jour. Geol. Soc. Japan*, 83: 573-580 (in Japanese with English abstract).

Tazaki, K., 1975. Chromian spinels in picrite basalts from Mineoka Tectonic Belt, Boso Peninsula, central Japan. *Jour. Geol. Soc. Japan*, 81: 399-406 (in Japanese with English abstract).

Terashima, S., 1971. Determination of cobalt, chromium, copper, lithium, nickel, lead, strontium and zinc in silicates by atomic absorption spectrometry. *Bull. Geol. Surv. Japan*, 22: 245-259 (in Japanese).

Terashima, S., 1973. Atomic absorption analyses of Be, V, Ba and Rb in rocks and flame emission analyses of Rb. *Bull. Geol. Surv. Japan*, 24: 469-485 (in Japanese).

Thompson, R.N., 1973. Titanian chromite and chromian titanomagnetite from a Snake River plain basalt, a terrestrial analogue to lunar spinels. *Am. Min.*, 58: 826-830.

Tiba, T., 1976. Hornblende megacrysts in andesite from Hakusan Volcano. *Bull. Natr. Sci. Mus., Ser. C (Geol.)*., 2(3): 115-119.

Togashi, S., 1977. Petrology of Osore-yama Volcano, Japan. *Jour. Japan Assoc. Min. Petr. Econ. Geol.*, 72: 45-60 (in Japanese with English abstract).

Tomita, T., 1935. On the chemical composition of the Cenozoic alkaline suite of the Circum-Japan Sea region. *Jour. Shanghai Sci. Inst.*, Sect. 2, 1: 227-306.

Treuil, M. and Varet, J., 1973. Critéres volcanologiques, pétrologiques et géochimiques de la genese et de la différenciation des magmas basaltiques: exemple de l'Afar. *Bull. Soc. Geol. Fr.*, 15: 401-644.

Ujike, O. and Onuki, H., 1976. Phenocrystic hornblendes from Tertiary andesites and dacite, Kagawa Prefecture, Japan. *Jour. Japan. Assoc. Min. Petr. Econ. Geol*, 71: 389-399.

Wager, L.R., Brown, G.M., and Wadsworth, W.J., 1960. Types of igneous cumulates. *Jour. Petr.*, 1: 73-85.

Whittaker, E.J.W. and Muntus, R., 1970. Ionic radii for use in geochemistry. *Geochim. Cosmochim. Acta*, 34: 945-956.

Yagi, K., 1959. Petrochemistry of the Cenozoic alkalic rocks of Japan and surrounding areas. *Bull. Volc. Soc. Japan*, 2nd Ser., 3: 63-75 (in Japanese).

Yamamoto, M., 1977. *Petrological study of Oshima-Ōshima Volcano* (MS). Master's Thesis, No. 107, Dept. Geol. Min., Fac. Sci., Univ. Hokkaido, 56 pp. (in Japanese).

Yamamoto, M., Katsui, Y., and Niida, K., 1977. Petrology of volcanic rocks and ultramafic-mafic inclusions of Oshima-Ōshima Volcano. *Bull. Volc. Soc. Japan, 2nd Ser., 22: 241-248 (in Japanese with English abstract).*

Yamamoto, M., 1978. Crystallization of the basaltic magma in Oshima-Ōshima Volcano. *Magma*, 45: 3-7 (in Japanese).

Yamazaki, T., Onuki, H. and Tiba, T., 1966. Significance of hornblende gabbroic inclusions in calc-alkali rocks. *Jour. Japan Assoc. Min. Petr. Econ. Geol.*, 55: 87-103.

Yoder, H.S. Jr., 1969. Experimental studies bearing on the origin of anorthosite. In: Isachsen (ed.), *Origin of Anorthosite and Related Rocks*, N.Y. State Mus. and Sci., Ser 18: 13-29.

Yusa, Y. and Tsuzuki, Y., 1979. Mutual transformation among α-factors for elements, oxide and some minerals. In: Min. Soc. Japan (ed.), *Studies on the chemical composition of minerals by electron probe microanalyser*: 93-100 (in Japanese).

(Manuscript received on Oct. 31, 1983; revised and accepted on Nov. 18, 1983)